Distributed Network of Coupled Oscillators with Multiple Limit Cycles

Kewei Ren and Tetsuya Iwasaki

***Abstract*—When designing feedback controllers to achieve periodic movements, a reference trajectory generator for oscillations is an important component. Using autonomous oscillators to this effect, rather than directly crafting periodic signals, may allow for systematic coordination in a distributed manner and storage of multiple motion patterns within the nonlinear dynamics, with potential extensions to adaptive mode switching through sensory feedback. This paper proposes a method for designing a distributed network that possesses multiple stable limit cycles from which various output patterns are generated with prescribed frequency, amplitude, temporal shapes, and phase coordination. In particular, we adopt, as the basic dynamical unit, a simple nonlinear oscillator with a scalar complex state variable, and derive conditions for their distributed interconnections to result in a network that embeds desired periodic solutions with orbital stability. We show that the frequencies and phases of target oscillations are encoded into the network connectivity matrix as its eigenvalues and eigenvectors, respectively. Various design examples will illustrate the proposed method, including generation of human gaits for walking and running.**

***Index Terms*—Nonlinear oscillator, distributed network, multistability, limit cycles, gait generation**

I. Introduction

A. Motivation

Periodic or oscillatory motions are essential in various engineering applications, including repetitive movement tasks for manipulators [1], periodic aircraft motion during cruising flight for improved fuel economy [2], [3], periodic trajectories for persistent monitoring by a single robot [4] or by a set of mobile agents [5], and oscillating body systems for ocean wave energy conversion [6]. To achieve periodic movements for a physical system, one could design a feedback regulator to track an oscillatory reference command. While such reference commands can be crafted as fixed time-dependent signals, it is often advantageous to use oscillators that autonomously generate periodic commands as stable limit cycles.

An advantage of using oscillators is that complex motion patterns[1] can be encoded into a single network. For example, multiple limit cycles may be embedded in the dynamics to allow for forced gait[2] transition from swimming to walking in robotic locomotion systems [7], [8]. Another advantage is the capability to modify the motion pattern autonomously when a reference oscillator is placed within the feedback loop. For instance, it is possible to adjust the periodic movements through sensory feedback in accordance with the change in the environmental condition [9]. Such adaptation mechanisms are found in biology — central pattern generators (CPGs) for animal locomotion [10]. Yet another advantage of autonomous oscillators in general is the fact that motion commands at multiple subsystems can be coordinated through local communications in a spatially distributed manner. A network of oscillators can be used as a distributed reference generator for designing control systems that are potentially robust against local failures [11]. Thus, a multi-pattern oscillator with distributed network architecture is of great interest as part of the control design.

More specifically, a general framework for feedback control design to achieve prescribed oscillations is given by Fig. 1. It has been proven for linear systems [12] that every controller that meets oscillatory design specifications for the closed-loop system must necessarily have the architecture in Fig. 1, where an autonomous oscillator (labeled as 'OSC') is embedded within the controller as an internal model, and is coupled with the plant diffusively (i.e., w converges to zero in the steady state). The oscillator is designed to autonomously (with $w = 0$) generate periodic signals u_s and y_s that are consistent with the input and output of the plant under the desired oscillation. Convergence to the desired oscillation pattern is guaranteed when the dynamical elements F and G are designed to stabilize some augmented plant.

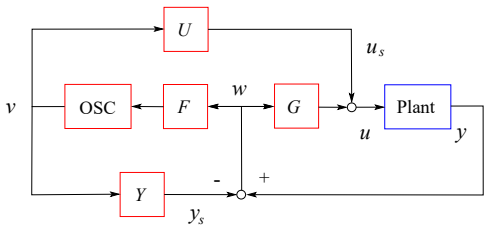

Fig. 1. General control architecture for oscillation

The framework in Fig. 1 may extend to nonlinear systems and provide a new paradigm for feedback control to achieve adaptive multi-pattern oscillations in a distributed manner. Indeed, the nonlinear neural control for locomotion in biology [10] exhibits a coupled CPG/plant architecture equivalent to the one in Fig. 1. Such design framework would be relevant especially for development of robotic locomotion systems that can adapt gaits with respect to environmental changes and are robust against electro-mechanical failures due to the distributed control architecture. The first step toward the new paradigm would be the design of multi-pattern, distributed, network oscillators to fill the role of 'OSC' in Fig. 1.

The authors are with the Department of Mechanical and Aerospace Engineering at University of California, Los Angeles, Los Angeles, CA 90095, USA. Emails: {kwren, tiwasaki}@ucla.edu.

[1]An oscillation pattern is a vector-valued periodic signal characterized by the period, amplitudes, phases, and temporal shapes of the variables.

[2]A gait is an oscillation pattern expressed by the vector of body shape variables for the purpose of locomotion.

B. Current State of the Art

The distributed network of dynamical subsystems has been extensively studied in the literature. The advances in design methods for consensus/synchronization of multi-agent systems offer a solid theoretical foundation using graph theory. Based on the dynamics of individual agents and the connectivity across agents, various theories have been developed for specific models. For example, the agents can be homogeneous [13]–[15] or heterogeneous [12], [16], [17], and each agent can be an independent oscillator [18] or a non-oscillatory subsystem that starts to exhibit a periodic trajectory if coupled properly with others [19], [20]. The coupling between agents may be linear [21] or nonlinear [22], and the coupling strength may be strong [23], [24] or weak [25], [26]. The design of coupled oscillators is similar to the formation control problem in that coordination of subsystems is achieved when the network graph is connected in some sense (e.g. containing a spanning tree [27]) and the coupling is properly designed. Typically, an internal model of the periodic target trajectory (without coordination) is already embedded in each local oscillator dynamics as in the consensus of integrator agents. A major difference is that coupled oscillator designs require orbital stability of limit cycles, making the problem challenging.

Effective methods have been established for the design of a distributed network oscillator with a single stable limit cycle. There are several representative methods for analyzing the coupling conditions for coordination of subsystems. One is the theory of contraction/semi-passivity [23], [24], [28]–[30]. This theory extends the Lyapunov stability criterion for an equilibrium to a flow-invariant subspace, ensuring global convergence to the synchronized state by strong coupling. While the method is powerful, it is not suitable for network design to achieve multiple limit cycles because each orbit must be stable only locally as global convergence to an orbit would imply non-convergence to any other orbits. Another method is the classical harmonic balance [31]. When the system consists of linear dynamics and static nonlinearities, the latter may be approximated by describing functions and the resulting quasi-linear system can be used to estimate stable limit cycles. This approach establishes the direct correspondence between the eigenstructure of the network and the oscillation profile [19], [32]. However, the existence and stability of limit cycles are not guaranteed due to the nature of harmonic approximation. A third method is based on linearization around a periodic orbit and the Floquet analysis [33]. When applied to synchronization of diffusively coupled homogeneous subsystems, the method gives a simple criterion for convergence in terms of the master stability function [34], [35]. The result extends to the coordination problem when the coupling is weak or the system exhibits flow invariance [26]. Yet another method is the phase reduction for weakly coupled oscillators. The Malkin theorem [36] or averaging techniques [25] allow for a description of the system in terms of phase variables, leading to the phase-coupled oscillators (PCOs) for which coordination problems reduce to stability analysis of equilibrium points [37]–[39].

For the design of an oscillator with multiple limit cycles, some of the methods mentioned above should be useful, but have not been fully explored in the literature. The problem has been well motivated and studied extensively in the context of gait transition for robotic locomotion systems. Most results focus on specific body configurations such as bipedal [40], quadruped [41], hexapod [42], undulatory [43], and hybrid [7], and design oscillator networks with a topology deduced from the symmetry considerations [44], [45]. Some of these provided systematic design methods based on dynamical systems theories. Strictly speaking, however, most of these results do not achieve multiple limit cycles with a fixed network condition, but rather the gait transition is induced through bifurcation with respect to a "drive" parameter that adjusts directly or indirectly the frequency and/or phase properties. Typically, the drive input is applied uniformly to all subsystems of the network, requiring a globally broadcasting command. In some cases, the bifurcation diagrams indicate coexistence of multiple stable limit cycles, which is considered to be an essential property of biological systems for switching between multiple coordination patterns [40], [44]. Multistability may allow fully autonomous mode transitions adapting to environmental changes through distributed local sensory feedback without relying on a global drive command [46], [47]. However, there is no systematic method for designing distributed network oscillators to achieve multiple limit cycles with a theoretical guarantee for orbital stability.

C. Contributions

In this paper, we will propose a rigorous design method to embed multiple limit cycles, with local orbital stability, in a fixed distributed network of dynamical subsystems, so that each limit cycle generates coordinated oscillatory outputs with prescribed frequency, amplitudes, phases, and temporal shapes. The network may be used in future developments to form the 'OSC' block in Fig. 1 as an internal model within a feedback controller, but our focus here is not on such control design but on the network oscillator design. Our approach considers a network of homogeneous basic units, each described by $\dot{z} = j\omega\psi(z)$ where the state variable $z(t) \in \mathbb{C}$ is a complex scalar and $\psi(z)$ is a static nonlinear function. The dynamical unit is a generalization of the Andronov-Hopf oscillator, and has a stable limit cycle with a circular orbit $z(t) = \gamma e^{j\omega t}$ on the complex plane. This choice of the unit oscillator is motivated by the fact that a periodic output of an arbitrary temporal shape can be generated approximately as a polynomial function of z using a finite Fourier series.

The general network of the unit oscillators is described by $\dot{z} = M\psi(z)$, where $z(t) \in \mathbb{C}^n$ is the complex state vector and $M \in \mathbb{C}^{n\times n}$ is the network connectivity matrix. The problem is to determine the structured matrix M and output function h so that desired periodic oscillations of arbitrary temporal shapes are generated in the output $y = h(z)$ from harmonic oscillations of z, embedded in the network as stable limit cycles. We will show how the output y can be defined as a function of z in a distributed manner, which is nontrivial because a single output function h must generate different prescribed shapes, depending on different harmonic limit cycles. Once this is done, the rest of the paper will focus on the network design for harmonic oscillations.

To lay a foundation for solving the multistability problem, we first consider the unstructured network design to embed a single limit cycle. We will take the linearization/Floquet approach to the orbital stability analysis. The coordination problem to set an arbitrary phase relationship between state variables is shown to be equivalent to the synchronization problem to set a common phase to all variables due to the flow-invariance of the unit oscillator. The necessary and sufficient condition for orbital stability of the synchronized oscillation is characterized in terms of the eigenvalues of a linear time-invariant system obtained through a time-varying Lyapunov transformation and linearization around the target orbit. Simple sufficient conditions are then obtained for three special cases of weak coupling, weak nonlinearity, and decoupled eigen-subsystems, in terms of the associated Laplacian matrix.

We then extend the development to the multiple ($\mathring{\imath} \geq 2$) limit cycle case. We start by examining the three conditions obtained for the single limit cycle case, and determine that the weak nonlinearity condition is most viable, providing a transparent condition in terms of the original connectivity matrix M. The same linearization technique is applied with respect to each of the $\mathring{\imath}$ limit cycles without transforming the problem to synchronization. Exploiting an eigenvalue perturbation result under sufficiently weak nonlinearity, we will show that every linearized system satisfies the condition for orbital stability if M has all the eigenvalues in the open left half plane except for $\mathring{\imath}$ eigenvalues $j\omega^i$ on the imaginary axis, where ω^i is the frequency of the i^{th} limit cycle and the corresponding eigenvector specifies the target phases.

Finally, we show how a distributed architecture can be imposed on the network. Such requirement is enforced by a constraint on the structure of the connectivity matrix M. Given an arbitrary network topology with the associated graph containing a spanning tree, it is easy to design a distributed network to embed a single limit cycle of desired oscillation profile [26], [30]. It turns out, however, that a direct extension to the multistability case is extremely difficult when the topological constraint is imposed on the connections between individual unit oscillators. We will show that the difficulty can be overcome by imposing the topological constraint on the connections between subsystems, each of which comprises (at least) $\mathring{\imath}$ unit oscillators. The overall design method will be illustrated by a comprehensive example to reproduce kinematic data from human walking and running as two stable limit cycles of a chain of oscillators distributed over ankle, knee, and hip joints of left and right legs. We will illustrate potential for gait transition as well as robustness against local failures.

In a preliminary version of this paper [48], with linear coupling of the unit oscillators, multiple limit cycles are embedded in an unstructured network. This method encodes the frequencies in the unit oscillator and phases in the network. As a result, undesired limit cycles with unintended combinations of the frequency and phase are stabilized in addition to desired ones. The present paper circumvents this adverse effect by encoding both frequencies and phases in the network through nonlinear coupling. Also, the temporal shaping of the output is new, and design examples are added to illustrate convergence properties, domain of attraction, gait transition, and robustness.

D. Notation

We use the following notation. The set of complex numbers with negative real parts is $\mathbb{C}^-$. Define $\mathbb{I}_n := \{1, 2, \cdots, n\}$ for a positive integer n, and $\emptyset$ denotes the empty set. For matrices V_k, $k \in \mathbb{I}_n$, let $V := \text{col}(V_1, \ldots, V_n)$ be the vertical concatenation of the arguments in a column, and $\text{diag}(V_1, \ldots, V_n)$ be the block diagonal matrix with the arguments on the diagonal, which may be abbreviated as $\text{diag}(V)$ when V_k are scalars. For a complex matrix $M \in \mathbb{C}^{m\times p}$, notations $\bar{M}$, $M^{\intercal}$, M^*, $M^\dagger$, $\Re(M)$, $\Im(M)$, and $\text{eig}(M)$ mean the complex conjugate, transpose, complex conjugate transpose, the Moore-Penrose inverse, real part, imaginary part, and the set of eigenvalues (when $m = p$), respectively. The real form of M is defined by $M^{\text{r}} := \left[\begin{smallmatrix} \Re(M) & -\Im(M) \\ \Im(M) & \Re(M) \end{smallmatrix}\right]$. The imaginary number is $j := \sqrt{-1}$. The Kronecker product is denoted by $\otimes$. Any scalar functions such as $\sin, \cos, \exp, |\cdot|$ are performed elementwise. For instance, $e^{j\theta}$ for $\theta \in \mathbb{R}^n$ is a vector with entries $e^{j\theta_k}$, where θ_k is the k^{th} entry of θ. Given a vector x and a scalar y, the operation $z = x + y$ is defined as the addition of y to each entry of x, namely $z_k = x_k + y$. For vectors $x, y \in \mathbb{C}^n$, $x \cdot y$ means the elementwise multiplication. For vector x and scalar l, the power x^l is taken elementwise. The vector with all entries equal to one is denoted by $\mathbf{1}$.

II. Design Framework for Coupled Oscillators

A. Basic Oscillator Unit

We will adopt, as a primitive computing unit, a nonlinear harmonic oscillator with a complex *scalar* variable as follows.

Lemma 1. *Let a function $\phi : \mathbb{R} \mapsto \mathbb{C}$ and real positive parameters γ and ω be given. Suppose $\phi(\alpha)$ is continuously differentiable in the neighborhood of $\alpha = \gamma$. Consider*

$$\dot{z} = j\omega\psi(z), \quad \psi(z) := \phi(|z|)z, \quad z(t) \in \mathbb{C}. \tag{1}$$

Then $z(t) = \zeta(t) := \gamma e^{j\omega t}$ is a solution if and only if $\phi(\gamma) = 1$. Suppose further that $\phi(\gamma) = 1$ and $\Im(\phi'(\gamma)) > 0$ hold, where ϕ' is the derivative of ϕ. Then, $z(t)$ converges to $\zeta(t+\tau)$ for some $\tau \in \mathbb{R}$ depending on $z(0) \in \mathbb{C}$ whenever $|z(0)|$ is sufficiently close to γ.

Proof. The result follows from Theorem 1 in [48] by redefining ϕ in the reference as $j\omega\phi$ here. ■

The essential part of oscillator (1) was introduced in [48] as a generalization of the Andronov-Hopf oscillator which has been used as a basis for expressing an arbitrary temporal shape using a Fourier series [49]. The following example illustrates how the unit oscillator (1) can be used to generate periodic signals with arbitrary shapes.

Example 1. Consider the system in (1) with

$$\phi(\alpha) = 1 + j\mu(\alpha^2 - \gamma^2), \quad \gamma = 1, \quad \mu > 0, \tag{2}$$

which is an Andronov-Hopf oscillator. Clearly, we have $\phi(\gamma) = 1$ and $\Im(\phi'(\gamma)) = 2\mu\gamma > 0$, and hence the local convergence of $z(t)$ to $\zeta(t+\tau)$ is guaranteed as in Lemma 1. We set $\mu = 0.2$. Suppose a target periodic signal is given by

$$\eta(t) = 3\cos(\omega t) + \cos(2\omega t) - \sin(4\omega t), \quad \omega = 5.$$

Then η can be expressed as

$$\eta = h(\zeta), \quad h(z) := \Re(3z + z^2 + jz^4).$$

Hence, defining the output $y := h(z)$, we can achieve convergence of $y(t)$ to $\eta(t+\tau)$ for some $\tau \in \mathbb{R}$ depending on the initial condition $z(0)$. The system is simulated with the initial condition $z(0) = \gamma/10$, which gives $\tau = 0$. The result is shown in Fig. 2. The real and imaginary parts of $z(t)$ converge to sinusoids, and output y converges to the non-sinusoidal signal of the specified shape.

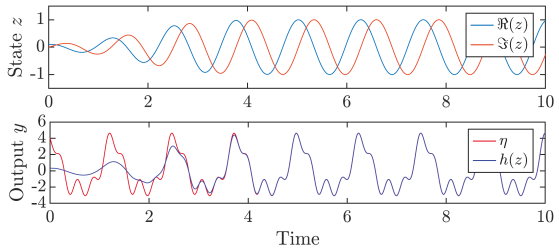

Fig. 2. Complex oscillator with non-sinusoidal temporal shape.

The example demonstrates potential of the simple oscillator (1) for various applications, including feedback control of periodic movements. We will use (1) as the basic unit for the network of oscillators studied in this paper. Based on Lemma 1, we introduce the following assumption which guarantees local convergence property $z(t) \to \zeta(t+\tau)$ for the oscillator in (1).

Assumption 1. The function $\phi : \mathbb{R} \mapsto \mathbb{C}$ is continuously differentiable in the neighborhood of $\gamma \in \mathbb{R}$ and satisfies

$$\phi(\gamma) = 1, \quad \phi'(\gamma) = j\varepsilon/\gamma, \tag{3}$$

for some $\varepsilon > 0$. The function $\psi : \mathbb{C} \mapsto \mathbb{C}$ is defined by $\psi(z) := \phi(|z|)z$.

For the rest of the paper, we make this a standing assumption imposed on every results. The assumption implicitly states that the real part of the derivative $\phi'(\gamma)$ is zero. This condition is not required for the local convergence but is imposed for simplicity.

B. Network of Oscillators with Nonlinear Coupling

Moving forward, we consider a coordination problem for a network of basic oscillators described in (1). In this network, each oscillator is a dynamical unit constituting a node. Without any communication between the units, the trajectory of an individual oscillator would locally converge to an oscillation of the prescribed frequency and amplitude, but the phase relationship between units is undetermined. We aim to achieve a phase coordination between units by properly designing the weights (coupling strengths and signs) of the network.

A general network of basic oscillators (1) is described by

$$\dot{z}_k = j\omega_k\psi(z_k) + \sum_{l=1}^{n} g_{kl}\psi(z_l), \quad z_k(t) \in \mathbb{C}, \quad k \in \mathbb{I}_n, \tag{4}$$

where n is the number of units, and $g_{kl} \in \mathbb{C}$ is the coupling parameter from the l^{th} unit to the k^{th} unit. The parameter $\omega_k \in \mathbb{R}$ is the intrinsic frequency of the k^{th} basic oscillator, but this value is irrelevant since we allow a nonzero value for g_{kk}. Thus a more compact description of the coupled basic oscillators is

$$\dot{z} = M\psi(z), \quad z(t) \in \mathbb{C}^n, \tag{5}$$

where $M \in \mathbb{C}^{n\times n}$ is the coupling matrix consisting of g_{kl} and ω_k. It should be noted that the couplings in (4) are nonlinear, unlike the linearly coupled Andronov-Hopf oscillators[3] considered in the literature [26], [30], [50]. It turns out that the nonlinearity of the couplings is important for encoding the oscillation frequency into the network, rather than into the individual oscillator unit. The use of the common nonlinearity ψ for the coupling and oscillator dynamics allows for the compact description in (5), which will facilitate the theoretical development.

Within this framework, we consider the set of $\mathring{\kappa}$ local subsystems of network oscillators

$$\dot{z}_k = F_k\psi(z_k), \quad z_k(t) \in \mathbb{C}^{n_k}, \quad k \in \mathbb{I}_{\mathring{\kappa}}, \tag{6}$$

that are coupled to each other in accordance with the network topology specified by the neighbor index sets $\mathbb{N}_k \subset \mathbb{I}_{\mathring{\kappa}}$ as

$$\dot{z}_k = F_k\psi(z_k) - \sum_{l\in\check{\mathbb{N}}_k} \ell_{kl}G_{kl}\psi(z_l), \quad k \in \mathbb{I}_{\mathring{\kappa}}, \tag{7}$$

where $F_k \in \mathbb{C}^{n_k\times n_k}$ specifies the local coupling between units in the same subsystem, $G_{kl} \in \mathbb{C}^{n_k\times n_l}$ specifies the connections from the l^{th} subsystem to the k^{th} subsystem, and $\check{\mathbb{N}}_k := \mathbb{N}_k \cup \{k\}$. The redundant parameter ℓ_{kl} and the negative sign are introduced to facilitate orbital stability analyses later.

The network of subsystems in (7) can be written as (5) with a structured matrix M defined by F_k and $\ell_{kl}G_{kl}$, where[4]

$$z := \operatorname{col}(z_1, \ldots, z_{\mathring{\kappa}}) \in \mathbb{C}^n, \quad z_k \in \mathbb{C}^{n_k}, \quad k \in \mathbb{I}_{\mathring{\kappa}}. \tag{8}$$

Here, the state vector z of the entire network is partitioned into z_k, which are vectors in general. Each subsystem can be deemed a cluster with states z_k. In the special case where an individual oscillator unit constitutes a subsystem ($n_k = 1$), we have $\mathring{\kappa} = n$, and z_k is the k^{th} scalar component of vector z.

C. Problem Formulation and Road Map

We are interested in oscillatory behaviors of the network system (5). Let us recall some basic concepts associated with oscillations that are needed for describing our objective precisely. Here we adopt the notion of orbital stability defined in e.g. [51].

Definition 1 (Orbital stability)**.** Let $z(t) = \zeta(t) \in \mathbb{C}^n$ be a periodic solution to an autonomous system $\dot{z} = f(z)$. The *orbit* of $\zeta(t)$ in the state space is the closed curve

$$\mathbb{O} := \{\zeta(t) \in \mathbb{C}^n : t \in \mathbb{R}\}.$$

[3]The linearly coupled Andronov-Hopf oscillators are given by (4) with $\psi(z_l)$ in the summation replaced by z_l.

[4]The partition of $(\cdot)$ associated with the k^{th} subsystem is denoted by $(\cdot)_k$.

Define the distance between vector $z \in \mathbb{C}^n$ and orbit $\mathbb{O}$ by

$$\mathrm{dist}(z, \mathbb{O}) := \inf_{\mathrm{o} \in \mathbb{O}} \|z - \mathrm{o}\|.$$

Then the solution ζ is said to be *orbitally stable* if (a) for each $\varepsilon > 0$, there exists $\delta > 0$ such that $\mathrm{dist}(z(0), \mathbb{O}) < \delta$ implies $\mathrm{dist}(z(t), \mathbb{O}) < \varepsilon$ for all $t \geq 0$, and (b) there exist positive scalars δ, c_1, and c_2 such that $\mathrm{dist}(z(0), \mathbb{O}) < \delta$ implies

$$\mathrm{dist}(z(t), \mathbb{O}) \leq c_1 e^{-c_2 t}, \quad \forall t \geq 0.$$

Note that we use the term *orbital stability* to mean local exponential convergence to the orbit. An orbitally stable solution, or its orbit, is referred to as a *stable limit cycle*. It is well known (e.g. Theorem 11.1, [52]) that orbital stability means convergence of $z(t)$, not to $\zeta(t)$, but to $\zeta(t+\tau)$ for some constant $\tau \in \mathbb{R}$.

The general goal is to design a distributed oscillator network containing multiple stable limit cycles in the state space. More specifically, we will solve the following:

Problem 1. Consider the dynamical network described by (5) where $M \in \mathbb{C}^{n \times n}$ is a constant matrix, and $n \geq 2$. Let desired oscillations be given by

$$\zeta^i(t) := \gamma e^{j(\omega^i t + \theta^i)} \in \mathbb{C}^n, \quad i \in \mathbb{I}_{\mathring{\imath}}, \tag{9}$$

where $\mathring{\imath} \geq 1$ is the number of the target oscillations, $\gamma, \omega^i \in \mathbb{R}$ are positive constants specifying the amplitude and frequencies, respectively, and $\theta^i \in \mathbb{R}^n$ are vectors specifying the phases.[5] Find the network interconnection matrix M such that $z = \zeta^i$, $i \in \mathbb{I}_{\mathring{\imath}}$ are stable limit cycles of system (5), and the network architecture is constrained to have the form (7), where $\mathring{\kappa}$ subsystems are interconnected with the network topology specified by neighbor sets $\mathbb{N}_k \subset \mathbb{I}_{\mathring{\kappa}}$ for $k \in \mathbb{I}_{\mathring{\kappa}}$.

The variables and parameters are summarized as follows:

n	total number of units in the network
n_k	number of units in the k^{th} subsystem
$k \in \mathbb{I}_{\mathring{\kappa}}$	indices for $\mathring{\kappa}$ subsystems
$i \in \mathbb{I}_{\mathring{\imath}}$	indices for $\mathring{\imath}$ target limit cycles
$\mathbb{N}_k \subset \mathbb{I}_{\mathring{\kappa}}$	index set for neighbors of k^{th} subsystem
$z(t) \in \mathbb{C}^n$	state vector of the network
$\zeta^i(t) \in \mathbb{C}^n$	target limit cycles $\zeta^i(t) = \gamma e^{j(\omega^i t + \theta^i)}$ $\gamma \in \mathbb{R}$, $\omega^i \in \mathbb{R}$, $\theta^i \in \mathbb{R}^n$

We will address Problem 1 through a sequence of subproblems in the order of increasing complexity with a preceding design forming a basis for the next design. The first subproblem, solved in Section III, is the design of all-to-all network (5) with a single limit cycle:

Problem 2. Solve Problem 1 with a single limit cycle ($\mathring{\imath} = 1$) without the network architecture constraint.

With the phase-shifted coordinates $r := \mathrm{diag}(e^{-j\theta^i})z$, the problem reduces to synchronization $r(t) \to \mathbf{1}e^{j\omega^i t}$, and an orbital stability condition will be given in terms of the network Laplacian matrix L (Theorem 1). This provides three possible design schemes and identifies the one suitable for extension to the second subproblem solved in Section IV, which is the design of (5) with multiple limit cycles:

Problem 3. Solve Problem 1 with possibly multiple limit cycles ($\mathring{\imath} \geq 1$) without the network architecture constraint.

Using the rotating frame $b^i := e^{-j\omega^i t} z$, the target limit cycles $z = \zeta^i$ become constants $b^i = \gamma e^{j\theta^i}$, and orbital stability is guaranteed by an eigenstructure property of M (Theorem 2). Finally, the network architecture constraint is imposed and Problem 1 is solved in Section V. Each subsystem F_k is designed by Theorem 1, and the inter-subsystem connections $\ell_{kl} G_{kl}$ will be specified so that M satisfies the eigenstructure condition in Theorem 2 and the distributed structure constraint via the Laplacian matrix (Theorem 3).

D. Temporal Shaping with Harmonics

Before proceeding to the design problems, this section describes how desired oscillations of arbitrary temporal shapes can be generated in a properly defined output $y(t) \in \mathbb{C}^m$ of the network oscillator (5). Given a set of (possibly anharmonic) periodic signals $\eta^i(t) \in \mathbb{R}^m$ for $i \in \mathbb{I}_{\mathring{\imath}}$, we will show how the harmonic target limit cycles $\zeta^i(t) \in \mathbb{C}^n$ and output function $y = h(z)$ can be chosen such that $\eta^i = h(\zeta^i)$ holds approximately. The result will motivate the design of nonlinear oscillators with harmonic orbits, and elucidate the value of the network oscillator design in the sections that follow.

Each of the $\mathring{\imath}$ target oscillations $\eta^i(t) \in \mathbb{R}^m$, $i \in \mathbb{I}_{\mathring{\imath}}$, can be described in terms of frequency $\omega^i \in \mathbb{R}$, phase $\varrho^i \in \mathbb{R}^m$, and temporal shape characterized by a 2π-periodic diagonal function $\mathfrak{s}^i : \mathbb{R}^m \mapsto \mathbb{R}^m$ as follows:

$$\eta^i(t) = \mathfrak{s}^i(\omega^i t + \varrho^i), \quad i \in \mathbb{I}_{\mathring{\imath}}. \tag{10}$$

For example, $\mathfrak{s}^i(\mathfrak{y}) := \gamma^i \sin \mathfrak{y}$ makes $\eta^i(t)$ sinusoidal with amplitude γ^i. The phase variable ϱ^i can be absorbed into the shape function $\mathfrak{s}^i$, but we keep this redundant description for design flexibility. When the temporal shape $\mathfrak{s}^i$ is piecewise continuous, it can be approximated by a finite Fourier series

$$\mathfrak{s}^i(\mathfrak{y}) \approx \sum_{l=0}^{\ell^i} \Re(c_l^i \cdot e^{jl\mathfrak{y}}), \quad c_l^i \in \mathbb{C}^m, \quad i \in \mathbb{I}_{\mathring{\imath}} \tag{11}$$

with arbitrary accuracy by taking a sufficiently large number of harmonics ℓ^i.

If the network (5) is designed to have $\mathring{\imath}$ limit cycles $z = \zeta^i$ that are harmonic with frequencies ω^i, then the desired output $y \approx \eta^i$ may be generated by shaping z appropriately. When there is a single desired oscillation ($\mathring{\imath} = 1$), the task is rather simple; one can use the Fourier series as illustrated in Example 1. However, the task is nontrivial when $\mathring{\imath} > 1$ since we need a single function h such that $h(\zeta^i) \approx \eta^i$ for all $i \in \mathbb{I}_{\mathring{\imath}}$. This requires a careful design of the output function h, which can be accomplished as follows.

Lemma 2. *Consider the $\mathring{\imath}$ signals $\eta^i(t) \in \mathbb{R}^m$ in (10) where the shape functions $\mathfrak{s}^i$ are exactly given by the right hand side*

[5] We use $(\cdot)^i$ to denote quantities related to the i^{th} target oscillation. To avoid confusion with power, we write $(\cdot)^2$ to mean $(\cdot)^i$ with $i = 2$.

of (11). Let $n \geq \mathring{\imath}$ *and* $\theta^i \in \mathbb{R}^n$ *for* $i \in \mathbb{I}_{\mathring{\imath}}$ *be given such that vectors* $e^{j\theta^i} \in \mathbb{C}^n$ *are linearly independent. Define*

$$h(z) := \sum_{i=1}^{\mathring{\imath}} \mathfrak{f}^i(H^i z), \quad \mathfrak{f}^i(\mathfrak{y}) := \sum_{l=0}^{\mathring{\varrho}^i} \Re(c_l^i \cdot \mathfrak{y}_l),$$

where $H^i \in \mathbb{C}^{m\times n}$ *are matrices such that*

$$H^i e^{j\theta^i} = e^{j\varrho^i}, \quad H^i e^{j\theta^{\check{\imath}}} = 0, \quad \forall\ \check{\imath} \neq i,$$

and $\mathfrak{y}_l := |\mathfrak{y}|$ *if* $l = 0$ *and* $\mathfrak{y}_l := \mathfrak{y}^l$ *otherwise. Then*

$$h(\zeta^i) = \eta^i, \quad \zeta^i(t) := e^{j(\omega^i t + \theta^i)}, \tag{12}$$

holds for all $i \in \mathbb{I}_{\mathring{\imath}}$.

Proof. The result follows by directly calculating $h(\zeta^i)$, noting that $H^i\zeta^i = e^{j(\omega^i t+\varrho^i)}$ and $H^i\zeta^{\check{\imath}} = 0$ for all $\check{\imath} \neq i$. To see that matrix $H^i \in \mathbb{C}^{m\times n}$ exists, note that it is constrained by

$$H^i E = D^i, \quad E := \begin{bmatrix} e^{j\theta^{\underline{1}}} & \cdots & e^{j\theta^{\mathring{\imath}}} \end{bmatrix}, \quad D := \begin{bmatrix} e^{j\varrho^{\underline{1}}} & \cdots & e^{j\varrho^{\mathring{\imath}}} \end{bmatrix},$$

where D^i is the matrix obtained from D by retaining the i^{th} column and replacing all the other columns by zeros. Since $e^{j\theta^i} \in \mathbb{C}^n$ for $i \in \mathbb{I}_{\mathring{\imath}}$ are linearly independent, E has a full column rank. Hence, existence of such H^i is guaranteed. ■

When $\mathring{\imath} = 1$, there are two representative schemes for the choice of H^i. One is the minimum-norm solution $H^i = D^i E^\dagger$. With $n = 1$, H^i is a vector and the desired shapes can be generated for all output channels from a single scalar variable $z(t) \in \mathbb{C}$. The other more distributed scheme would be to choose $n = m$, $\theta^i = \varrho^i$, and $H^i = I$. In this case, the k^{th} output y_k is created by shaping the k^{th} variable z_k.

When $\mathring{\imath} > 1$, a combination of the above two schemes would provide a reasonable choice of H^i. In particular, we partition the output into $y = \text{col}(y_1, \ldots, y_{\mathring{\kappa}})$ with $y_k \in \mathbb{R}^{m_k}$, $k \in \mathbb{I}_{\mathring{\kappa}}$, and consider $\mathring{\kappa}$ subsystems with states $z_k(t) \in \mathbb{C}^{n_k}$ where $n_k \geq \mathring{\imath}$. Partition the phase vectors θ^i and ϱ^i into $\theta^i_k \in \mathbb{R}^{n_k}$ and $\varrho^i_k \in \mathbb{R}^{m_k}$, accordingly. Here, θ^i_k are chosen so that $e^{j\theta^i_k}$ for $i \in \mathbb{I}_{\mathring{\imath}}$ are linearly independent. Then H^i can be chosen as $H^i = \text{diag}(D^i_1 E^\dagger_1, \ldots, D^i_{\mathring{\kappa}} E^\dagger_{\mathring{\kappa}})$ where D^i_k and E_k are defined in terms of ϱ^i_k and θ^i_k in a manner similar to D^i and E. This choice of H^i gives diagonal h that defines $y_k = h_k(z_k)$, and reduces to the first scheme of the $\mathring{\imath} = 1$ case if $\mathring{\kappa} = 1$, and to the second scheme if $n_k = m_k = 1$ and $\theta^i_k = \varrho^i_k$.

With Lemma 2, the output signal $y = h(z)$ satisfies $y(t) \to \eta^i(t + \tau)$ for some $\tau \in \mathbb{R}$ approximately when $z(t)$ converges to the orbit of $\zeta^i(t)$. Therefore, the rest of the paper will focus on the design of an oscillator network with complex state variables $z(t) \in \mathbb{C}^n$ to embed multiple harmonic oscillations ζ^i of the form (12) as stable limit cycles. The shaping scheme in this section will be illustrated by a design example in Section VI.

III. Single Limit Cycle Design

A. Approach

We consider the design of the nonlinear dynamical network (5) to embed a single limit cycle, i.e., Problem 2. We will omit superscript i since $\mathring{\imath} = 1$, and denote the target oscillation by

$$\zeta(t) := \gamma e^{j(\omega t+\theta)} \in \mathbb{C}^n. \tag{13}$$

Our approach to solving Problem 2 is the following. First, we will reformulate the problem as synchronization of coupled oscillators via a coordinate transformation. This allows for a proper characterization of the network connectivity in terms of a Laplacian matrix representing a diffusive coupling. Conditions for synchronization will then be obtained on the Laplacian matrix through linearization and the Floquet analysis, justified by a classical result on orbital stability [33].

B. An Equivalent Synchronization Problem

All entries of the target oscillation vector $\zeta(t) \in \mathbb{C}^n$ in (13) share the same amplitude $\gamma \in \mathbb{R}$ and frequency $\omega \in \mathbb{R}$, and differ only by the phases $\theta \in \mathbb{R}^n$. This motivates us to consider the following coordinate transformation

$$r := \Theta^* z, \quad \Theta := \text{diag}(e^{j\theta}), \quad r(t) \in \mathbb{C}^n. \tag{14}$$

The system (5) is then described as

$$\dot r = j\omega\psi(r) - L\psi(r), \quad L := j\omega I - \Theta^* M \Theta, \tag{15}$$

with the target limit cycle $r = \rho$ where

$$\rho(t) := \gamma \mathbf{1} e^{j\omega t} \in \mathbb{C}^n.$$

The first term in (15) is a collection of the unit oscillators $\dot r_k = j\omega\psi(r_k)$, each admitting a harmonic solution with specified amplitude γ and frequency ω, but an arbitrary phase when isolated. The second term specifies the coupling between oscillators, imposing a phase relationship across units. Note that all the variables $r_k(t) \in \mathbb{R}$ with $k \in \mathbb{I}_n$ are required to converge to each other. Thus, Problem 2 is equivalent to synchronization of the unit oscillators $\dot r_k = j\omega\psi(r_k)$ through the couplings specified by matrix L. Since there is a one-to-one correspondence between L and M, the coupling matrix L can be considered to be the design parameter.

The synchronization necessitates that L is a Laplacian matrix with the row sum equal to zero. That is, $r = \rho$ is a solution if and only if $L\mathbf{1} = 0$ holds, which can be verified by direct substitution. In this case, the system is described as

$$\dot r_k = j\omega\psi(r_k) + \sum_{l=1}^{n} \ell_{kl}\Big(\psi(r_k) - \psi(r_l)\Big), \quad k \in \mathbb{I}_n,$$

where ℓ_{kl} is the (k, l) entry of L, and we noted that the sum of ℓ_{kl} over $l \in \mathbb{I}_n$ is zero for each $k \in \mathbb{I}_n$. It is now clearly seen that the couplings are diffusive, i.e., each term in the summation becomes zero when the oscillators are synchronized.

C. Exact Condition for Orbital Stability

This section presents a necessary and sufficient condition for the network system (15) to have $r = \rho$ as a stable limit cycle. The condition is given on the Laplacian matrix L, which in turn provides a condition on the original connectivity matrix M, thereby solving Problem 2. The result is stated as follows.

Lemma 3. *Consider Problem 2. Define matrix L by (15) with Θ in (14). The periodic signal $\zeta(t)$ in (13) is a solution of (5) if and only if $L\mathbf{1} = 0$ holds. In this case, it is orbitally stable if and only if the eigenvalues of the following matrix are in the open left half plane except for one at the origin:*

$$\mathsf{A} := -\begin{bmatrix} L_R & -L_I \\ L_I & L_R \end{bmatrix} - \varepsilon \begin{bmatrix} \omega I - L_I & 0 \\ L_R & 0 \end{bmatrix} \tag{16}$$

where $L_R := \Re(L)$, $L_I := \Im(L)$, and ε defined by (3) dictates the local strength of the nonlinearity in the system (5).

Proof. With a coordinate transformation $r := \Theta^* z$, the system (5) is described by (15), and hence the problem reduces to the orbital stability analysis of $r = \rho := \Theta^* \zeta$. By construction, $z = \zeta$ in (13) is a solution of (5) if and only if $r = \rho$ is a solution of (15), which holds when $L\mathbf{1} = 0$. From a fundamental result (Theorem 1.1 in [51]), the solution $r = \rho$ is an orbitally stable limit cycle of (15) if and only if the Floquet multipliers of its linearization around $r = \rho$ are all strictly inside the unit circle except for one at 1.

To analyze the dynamics in the neighborhood of $r = \rho$, let $p := r - \rho$ and consider the linear approximations

$$\begin{aligned} &|r_k| = |p_k + \rho_k| = |p_k e^{-j\omega t} + \gamma| \approx \gamma + \Re(p_k e^{-j\omega t}), \\ &\phi(|r_k|) \approx \phi(\gamma) + \phi'(\gamma)\Re(p_k e^{-j\omega t}) = 1 + j(\varepsilon/\gamma)\Re(p_k e^{-j\omega t}), \\ &\psi(r_k) \approx p_k + \psi(\rho_k) + j(\varepsilon/\gamma)\Re(p_k e^{-j\omega t})\rho_k, \end{aligned}$$

where we used Assumption 1, and the second and higher order terms of p are ignored (here, the subscript k denotes the k^{th} entry of a vector). The linearization of (15) is then given by the periodically time-varying system

$$p := r - \rho, \quad \dot{p} = (j\omega I - L)\big(p + j\varepsilon \Re(p e^{-j\omega t}) e^{j\omega t}\big). \tag{17}$$

For a tractable characterization of the Floquet multipliers, we introduce a state coordinate transformation $q = pe^{-j\omega t}$, motivated by the fact that this transformation on r makes the target a constant solution $\rho(t)e^{-j\omega t} = \gamma\mathbf{1}$. This leads to the linear time-invariant system

$$q := pe^{-j\omega t}, \quad \dot{q} = -Lq + j\varepsilon(j\omega I - L)\Re(q). \tag{18}$$

Expressing this system in terms of the real state variable,

$$\mathsf{q} := \operatorname{col}(\Re(q), \Im(q)), \quad \dot{\mathsf{q}} = \mathsf{A}\mathsf{q} \tag{19}$$

is obtained, where $\mathsf{A} \in \mathbb{R}^{2n \times 2n}$ is defined in (16), using Lemma 5 in the appendix.

Since the state variables p and q are related by a Lyapunov transformation $p = qe^{j\omega t}$, the Floquet multipliers of (17) coincide with those of (19), which are equal to the eigenvalues of $e^{\mathsf{A}T}$ where $T := 2\pi/\omega$. Thus the Floquet multipliers are given by $e^{\lambda T}$ with λ being the eigenvalues of A. Hence, the orbital stability condition is given by $\Re(\lambda) < 0$ for all eigenvalues of A except for a simple eigenvalue at $\lambda = 0$. ■

Recall that the orbital stability means convergence of $z(t)$ to $\zeta(t + \tau)$ for some $\tau \in \mathbb{R}$. The time shift τ depends on the initial state, which is reflected by the condition that one of the eigenvalues of A is at the origin. When the nonlinearity is absent, i.e., $\phi(\alpha) = 1$ for all $\alpha \in \mathbb{R}$, the derivative $\phi'(\gamma)$ is zero and $\varepsilon = 0$. In this case, the eigenvalue of A at the origin is repeated at least twice since $L\mathbf{1} = 0$ holds and the eigenvalues of A are those of L and their complex conjugates due to Lemma 5. Thus, the second term in (16) resulting from the local nonlinearity at $\alpha = \gamma$ is essential for orbital stability.

While it is easy to check orbital stability by calculating the eigenvalues of A, it is not clear how the result in Lemma 3 for the single limit cycle case can be extended to enable the coupled oscillator design for multiple limit cycles. To gain further insights and allow for such extension, we will derive simple sufficient conditions for orbital stability in terms of the Laplacian matrix L in the next section.

D. Sufficient Conditions for Orbital Stability

Our approach to simplify the orbital stability condition is to consider small perturbations of some characteristic parameters. Let us introduce a parameter $\delta \in \mathbb{R}$ by replacing L by δL in (15), so that the original connectivity matrix M is parametrized as

$$M = j\omega I - \delta \Theta L \Theta^*. \tag{20}$$

In this case, A in (16) is modified by replacing L_R and L_I by δL_R and δL_I, and thus depends on δ and ε in addition to L. The parameter δ represents the strength of coupling between basic oscillators, while ε represents the strength of nonlinearity ψ in the neighborhood of the target orbit.

We seek sufficient conditions on L such that A satisfies the eigenvalue property for orbital stability described in Lemma 3 when one of the parameters δ and ε is sufficiently small, using an eigenvalue sensitivity result (Lemma 6 in the appendix). We also obtain a stronger condition on L when ε and δ are not necessarily small. The result is given as follows.

Theorem 1. *Consider Problem 2 with the dynamical network (5), where the connectivity matrix M is parametrized as (20) in terms of real positive scalar δ and complex matrix L. The periodic signal ζ in (13) is a stable limit cycle of (5) if one of the following conditions hold:*

(i) *Weak nonlinearity: $L \in \mathbb{L}$ and ε is sufficiently small,*
(ii) *Weak coupling: $\Re(L) \in \mathbb{L}$ and δ is sufficiently small,*
(iii) *Decoupling: $\Re(L) \in \mathbb{L}$ and $\Im(L) = 0$,*

where $\mathbb{L}$ is the set of complex square matrices L such that $L\mathbf{1} = 0$ and all its eigenvalues have positive real parts except for a simple eigenvalue at the origin.

Proof. Let $Q \in \mathbb{R}^{n \times (n-1)}$ be a matrix such that $\mathbf{1}^\intercal Q = 0$ and $Q^\intercal Q = I$. It can be shown, with constraint $L\mathbf{1} = 0$, that

$$\mathsf{A}W = W\Omega,$$

where A is defined in (16) and

$$W := \begin{bmatrix} \mathbf{1} & 0 & Q & 0 \\ 0 & \mathbf{1} & 0 & Q \end{bmatrix}, \quad \Omega := \begin{bmatrix} -\varepsilon\omega & 0 & * \\ 0 & 0 & * \\ 0 & 0 & \mathcal{D} \end{bmatrix},$$
$$\mathcal{D} := (Q^{\mathrm{r}})^\intercal \mathsf{A} Q^{\mathrm{r}}$$

Thus two eigenvalues of A are $-\varepsilon\omega$ and 0, and due to Lemma 3, the solution ζ is orbitally stable if and only if $\mathcal{D}$ is Hurwitz. Note that

$$\mathcal{D} = -\delta D^{\mathrm{r}} - \varepsilon \begin{bmatrix} \omega I - \delta D_I & 0 \\ \delta D_R & 0 \end{bmatrix} \tag{21}$$

where D_R, D_I and D are defined by

$$D := Q^{\mathsf{T}} L Q, \quad D_R := \Re(D), \quad D_I := \Im(D).$$

We prove the orbital stability exploiting the structure of $\mathcal{D}$.

Consider condition (i). When $L \in \mathbb{L}$, we have

$$\begin{bmatrix} \mathbf{1}^{\mathsf{T}}/n \\ Q^{\mathsf{T}} \end{bmatrix} L \begin{bmatrix} \mathbf{1} & Q \end{bmatrix} = \begin{bmatrix} 0 & * \\ 0 & D \end{bmatrix}. \tag{22}$$

and hence $-D$ is Hurwitz due to similarity between L and the right hand side. By Lemma 5 in the appendix, $-D^{\mathrm{r}}$ is also Hurwitz. It then follows from continuity of eigenvalues that $\mathcal{D}$ is Hurwitz when ε is sufficiently small.

Next consider (ii). Rewrite $\mathcal{D}$ as

$$\mathcal{D} = \mathcal{D}_A + \delta \mathcal{D}_B,$$

where

$$\mathcal{D}_A = \begin{bmatrix} -\varepsilon\omega I & 0 \\ 0 & 0 \end{bmatrix}, \quad \mathcal{D}_B = -D^{\mathrm{r}} + \varepsilon \begin{bmatrix} D_I & 0 \\ -D_R & 0 \end{bmatrix}.$$

Clearly, eigenvalues of $\mathcal{D}_A$ are $-\varepsilon\omega$ and 0, and the left and right eigenvectors associated with the latter are given by the columns of Y_1 and X_1, respectively, where $X_1 = Y_1 = \mathrm{col}(0, I) \in \mathbb{R}^{2n\times n}$. From Lemma 6, the n eigenvalues at the origin move to the open left half plane with sufficiently small $\delta > 0$ if $Y_1^* \mathcal{D}_B X_1 = -D_R$ is Hurwitz, which is the case when $\Re(L) \in \mathbb{L}$ due to (22) where $\Re(D) = D_R$.

Finally, consider (iii). Since L is real, we have $L_I = 0$ and $L_R = L$. It follows that $D_I = 0$ holds and $\mathcal{D}$ then becomes

$$\mathcal{D} = \begin{bmatrix} -\delta D_R - \varepsilon\omega I & 0 \\ -\varepsilon\delta D_R & -\delta D_R \end{bmatrix}.$$

Since $\mathcal{D}$ is block triangular, its eigenvalues are those of $-\delta D_R$ and $-\delta D_R - \varepsilon\omega I$. Both of these matrices are Hurwitz if $-D_R$ is Hurwitz, which is the case when $L \in \mathbb{L}$. ■

Weakly coupled oscillators have been extensively studied in the literature but the vast majority has focused on the analysis (rather than design) of Kuramoto-type phase coupled oscillators [37]–[39]. Our result (statement (ii) in Theorem 1) is one of the few that provide design conditions for synchronization of limit cycle oscillators. The result is new, but similar methods for proving orbital stability had been used in the literature to obtain results in different settings [21], [26].

Condition (iii) in Theorem 1 is labeled as "Decoupling" since the condition can also be derived from decoupling of the network system (15) into individual subsystems, with the coupling effect captured by the eigenvalues of the Laplacian matrix L. This decoupling approach is called the master stability analysis [34], to which our result relates as follows. Let a permutation of q in (19) be defined by

$$\hat{\mathsf{q}} := \mathrm{col}(\hat{\mathsf{q}}_1, \ldots, \hat{\mathsf{q}}_n), \quad \hat{\mathsf{q}}_k := \begin{bmatrix} \Re(q_k) \\ \Im(q_k) \end{bmatrix}.$$

With L being real, the system (19) is then described as

$$\begin{aligned} &\dot{\hat{\mathsf{q}}} = -\hat{\mathsf{A}}\hat{\mathsf{q}}, \quad \hat{\mathsf{A}} := I \otimes E + (L \otimes I)(I \otimes F), \\ &E := \begin{bmatrix} \varepsilon\omega & 0 \\ 0 & 0 \end{bmatrix}, \quad F := \begin{bmatrix} 1 & 0 \\ \varepsilon & 1 \end{bmatrix}. \end{aligned} \tag{23}$$

Let $L = V\Lambda V^{-1}$ be the spectral decomposition of L where $\Lambda := \mathrm{diag}(\lambda_1, \ldots, \lambda_n)$. Then, by the coordinate transformation $\hat{\mathsf{q}} = (V \otimes I)\mathsf{x}$, the system is block-diagonalized to become

$$\dot{\mathsf{x}}_k = -(E + \lambda_k F)\mathsf{x}_k, \quad \mathsf{x}_k(t) \in \mathbb{R}^2, \quad k \in \mathbb{I}_n.$$

Note that the eigenvalues of $E + \lambda_k F$ are λ_k and $\lambda_k - \varepsilon\omega$, and the collection of these for $k \in \mathbb{I}_n$ gives the eigenvalues of A. Hence, condition (iii) implies that the real parts are all negative except for one derived from $\lambda_k = 0$, leading to the orbital stability condition in Lemma 3.

In Theorem 1, the condition on L is the strongest for (iii), implying those for (i) and (ii), which makes sense since (iii) requires no additional property on ε or δ. These conditions have different implications on the Floquet exponents, i.e., the eigenvalues of A in (16), which dictate the rate of local convergence to the target orbit. We see from the proof that, for each case, two of the Floquet exponents are exactly at 0 and $-\varepsilon\omega$, and the remaining $2n-2$ are at

(i)	$-\lambda_k$,	$-\bar{\lambda}_k$,	(approximately with small ε)
(ii)	$-\varepsilon\omega$,	0,	(approximately with small δ)
(iii)	$-\lambda_k$,	$-\varepsilon\omega - \lambda_k$,	(exactly),

where λ_k for $k \in \mathbb{I}_{n-1}$ are the nonzero eigenvalues of δL, and each of $-\varepsilon\omega$ and 0 in (ii) is repeated $n-1$ times.

When L is real as in condition (iii), all of the $2n-1$ nonzero Floquet exponents can be placed away from the imaginary axis for faster local convergence by proper choices of the design parameters L and ε. When the nonlinearity is weak (small ε) as in (i), all nonzero Floquet exponents are approximately set by the network connectivity L except for one at $-\varepsilon\omega$. The state variable associated with the mode $-\varepsilon\omega$ is the average of the entries of $\Re(q)$, which is essentially the deviation of the average amplitude from γ. Hence, the convergence to the synchronized state can be fast if L is chosen so that its nonzero eigenvalues are far away from the imaginary axis, but the amplitude convergence can be slow if ε is close to zero. When the coupling is weak (small δ) as in (ii), $n-1$ Floquet exponents are close to the origin. These modes slow down convergence of $Q^{\mathsf{T}}\Im(q)$, which relates to synchronization of the phases, provided the n modes at $-\varepsilon\omega$ associated with the amplitudes are fast. The following example illustrates the discussion in this paragraph and shows how the parameters (δ, ε) affect the convergence behavior.

Example 2. Consider a network of three ($n = 3$) oscillators described by (5) with M given by (20). The target orbit is specified as (13) with $\omega = 2\pi$, $\gamma = 1$, and $\theta = \mathrm{col}(0, 0, \pi/2)$. For this study, the network connections are specified by

$$\begin{aligned} &L = L_R + jL_I, \\ &L_R = \begin{bmatrix} 1 & 0 & -1 \\ -1 & 2 & -1 \\ 0 & -1 & 1 \end{bmatrix}, \quad L_I = \begin{bmatrix} 2 & 0 & -2 \\ 1 & 3 & -4 \\ -1 & -7 & 8 \end{bmatrix}, \end{aligned}$$

where $L \in \mathbb{L}$ and $\Re(L) \in \mathbb{L}$. From Lemma 3, the target solution ζ is orbitally stable when the maximum real part of the eigenvalues of A in (16), excluding the one at the origin, is strictly negative. Some contours of this value are plotted on the (δ, ε) plane in Fig. 3(f), where the stability region is the area under the red curve. We chose several values of (δ, ε) as indicated by the stars and simulated the resulting network with the initial condition $z(0) = \mathrm{col}(1, -1, 0)/10$. The real parts of the state variables z_1, z_2, and z_3 are plotted in Fig. 3(a)–(e).

In case (a), ε is small and $L \in \mathbb{L}$, satisfying condition (i) for orbital stability in Theorem 1. The amplitude convergence is slow due to small ε. In case (b), δ is small and $\Re(L) \in \mathbb{L}$, satisfying condition (ii). The phase convergence is slow due to small δ. The convergence of both amplitude and phase can be made faster by choosing larger values of (δ, ε) as in case (c). We note from (f) that the maximum real part for (c) is no more negative than those for (a) and (b), and thus the local convergence rate deduced from the linearized system is not always indicative of the actual settling time. If (δ, ε) are made too large and placed above the red boundary in (f), the orbital stability is lost as shown in case (d). However, for the same large values of (δ, ε), the orbital stability is recovered when the imaginary part of L is set to zero as seen in case (e) due to satisfaction of condition (iii) in Theorem 1.

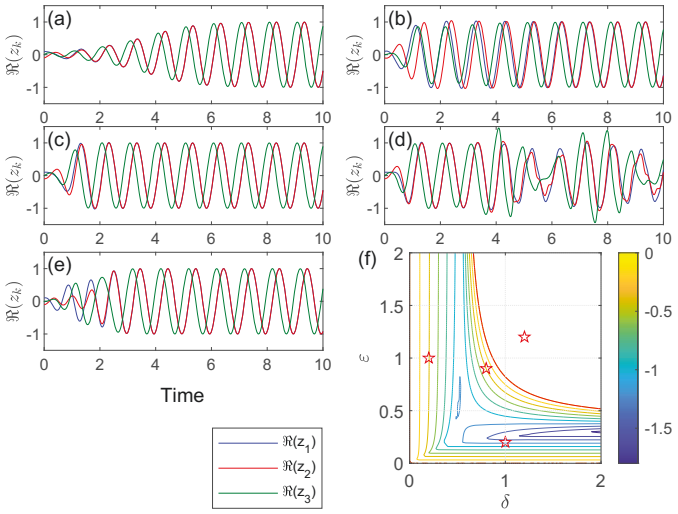

Fig. 3. Simulated responses the oscillator network with a single limit cycle. (a) $(\delta, \varepsilon) = (1, 0.2)$, (b) $(\delta, \varepsilon) = (0.2, 1)$. (c) $(\delta, \varepsilon) = (0.8, 0.9)$. (d) $(\delta, \varepsilon) = (1.2, 1.2)$. (e) $(\delta, \varepsilon) = (1.2, 1.2)$, with real L. (f) Contours of the maximum real part of the nonzero eigenvalues of A. The orbital stability is achieved in the region under the red curve. The stars indicate the four cases of (δ, ε).

IV. Multiple Limit Cycle Design

A. Approach

We now consider the design of the network (5) to embed multiple limit cycles, i.e., Problem 3. A natural approach to solving this problem would be to use Lemma 3 as a basis for establishing orbital stability of each target oscillation ζ^i. While it is easy to write down the condition for orbital stability, a difficulty stems from the fact that L in (15) depends on the particular orbit ζ^i through θ^i, and so does A in (16). Hence, it is not clear how to construct a single matrix M satisfying the multiple stability conditions. We will overcome this difficulty by turning our attention to the sufficient conditions for orbital stability in Theorem 1.

First, we exclude the decoupling condition (iii) from our consideration because the requirement $\Im(L) = 0$ is too restrictive. For each target orbit, n^2 scalar constraints will be imposed on M due to $\Im(L) = 0$ with L in (15), in addition to $L \in \mathbb{L}$. Therefore, the design freedom captured by the $2n^2$ real scalars in $M \in \mathbb{C}^{n \times n}$ may not be enough to satisfy the constraints when there are multiple target orbits. Next, we also exclude the weak coupling condition (ii) from our consideration. This is because weak coupling allows for phase coordination among oscillators, but the intrinsic frequency and amplitude of the individual, isolated oscillators will be preserved (or slightly perturbed) under weak coupling [25]. Hence, weakly coupled oscillators are not suitable for the design of a network with multiple limit cycles with various frequencies. Thus we will pursue remaining condition (i).

To gain insights, let us express condition (i) in Theorem 1 equivalently in terms of the original connectivity matrix M.

Corollary 1. *Consider Problem 2 with the dynamical network (5). The periodic signal ζ in (13) is a stable limit cycle if*

$$Mv = j\omega v, \quad \mathrm{eig}(M) \backslash \{j\omega\} \subset \mathbb{C}^-, \quad v := e^{j\theta} \in \mathbb{C}^n$$

holds, and ε defined in (3) is sufficiently small.

Proof. The orbital stability condition follows from Theorem 1 as it is equivalent to its statement (i). From (20), we have

$$\delta \Theta L = (j\omega I - M)\Theta.$$

Multiplying $\mathbf{1}$ from right and noting that $v = \Theta \mathbf{1}$, we see that $L\mathbf{1} = 0$ is equivalent to $j\omega v = Mv$. Also, (20) gives

$$\delta L = \Theta^* (j\omega I - M)\Theta$$

and hence $\mathrm{eig}(\delta L) = j\omega - \mathrm{eig}(M)$ by the similarity transformation. Thus $L \in \mathbb{L}$ holds if and only if the eigenvalues of M have negative real parts except for the one at $j\omega$. ■

A direct application of Corollary 1 to each target oscillation is not useful for solving Problem 3 with $\mathring{\imath} \geq 2$ since the condition would require M to have eigenvalues at $j\omega^i$ for $i \in \mathbb{I}_{\mathring{\imath}}$ while all eigenvalues except for one have to be in $\mathbb{C}^-$, which is always infeasible. However, since Corollary 1 gives a sufficient condition, it may be possible to relax the condition and still maintain sufficiency for orbital stability. Conditions

$$Mv^i = j\omega^i v^i, \quad v^i := e^{j\theta^i} \in \mathbb{C}^n, \quad i \in \mathbb{I}_{\mathring{\imath}} \tag{24}$$

are necessary for the target orbits ζ^i to be solutions of (5), and cannot be relaxed. Hence, the most reasonable relaxation would be to require the $n - \mathring{\imath}$ eigenvalues of M, other than $j\omega^i$ with $i \in \mathbb{I}_{\mathring{\imath}}$, to be in the open left half plane. We will show that the relaxed condition is indeed sufficient for orbital stability of the multiple limit cycles.

B. Conditions for Orbital Stability

Since converting to a synchronization problem would not help to solve the multiple limit cycle problem, we step back to the original coordinate, and derive the orbital stability condition in terms of the connectivity matrix M rather than the Laplacian matrix L. The result is as follows.

Lemma 4. *Consider Problem 3. The periodic signals $\zeta^i(t)$ in (9) are solution of (5) for all $i \in \mathbb{I}_{\bar{i}}$ if and only if (24) holds. In this case, the solutions are orbitally stable if and only if*

$$\mathsf{A}^i := \mathsf{M} - \omega^i \mathsf{J} + \varepsilon \mathsf{J}\mathcal{M}\mathsf{G}^i, \quad i \in \mathbb{I}_{\bar{i}}, \tag{25}$$

has all the eigenvalues in the open left half plane except for one at the origin, where

$$\mathsf{M} := M^{\mathrm{r}}, \quad \mathsf{J} := (jI)^{\mathrm{r}},$$
$$\mathsf{G}^i := \begin{bmatrix} C^i \\ S^i \end{bmatrix} \begin{bmatrix} C^i & S^i \end{bmatrix}, \quad \begin{matrix} C^i := \mathrm{diag}(\cos\theta^i), \\ S^i := \mathrm{diag}(\sin\theta^i). \end{matrix}$$

Proof. The signal ζ^i in (9) is a solution of (5) when

$$\dot{\zeta}^i - M\psi(\zeta^i) = \gamma(j\omega^i I - M)e^{j\theta^i}e^{j\omega^i t} = 0$$

holds for all $t \in \mathbb{R}$, where we noted $\psi(z) = z$ when $|z| = \gamma$ due to Assumption 1. This condition holds for all $i \in \mathbb{I}_{\bar{i}}$ if and only if (24) is satisfied. With a Lyapunov transformation $b^i := ze^{-j\omega^i t}$, the system (5) is described as

$$\dot{b}^i = M\psi(b^i) - j\omega^i b^i,$$

and the target oscillation $z = \zeta^i$ is transformed to $b^i = \beta^i$ where $\beta^i := \gamma e^{j\theta^i}$. Following a procedure similar to the proof of Lemma 3, we obtain the linearization around $b^i = \beta^i$ as

$$w^i := b^i - \beta^i, \quad \dot{w}^i = (M - j\omega^i I)w^i + j\varepsilon M\Theta^i \Re((\Theta^i)^* w^i),$$

where $\Theta^i := \mathrm{diag}(e^{j\theta^i})$. Defining the real state vector $\mathcal{w}^i := \mathrm{col}(\Re(w^i), \Im(w^i))$ and using Lemma 5, the system can be described as $\dot{\mathcal{w}}^i = \mathsf{A}^i \mathcal{w}^i$, where we note that $\Theta^i = C^i + jS^i$. Hence, by Theorem 1.1 in [51], the solution $z = \zeta^i$ is orbitally stable if and only if all the eigenvalues of A^i, except for one at the origin, have negative real parts. ■

The condition in Lemma 4 is useful for stability analysis of the multiple limit cycles ζ^i when system (5) is given. However, it does not give a constructive method for designing M satisfying the condition. Hence, we build on this result and proceed to obtain a sufficient condition directly useful for the design. Based on the observations in the previous section, we consider the case where ε is small, i.e., the nonlinearity in the basic oscillator is weak. The problem then boils down to the perturbation analysis of the eigenvalues of A^i, which can be addressed by Lemma 6, and the result is as follows.

Theorem 2. *Consider Problem 3 with the dynamical network (5). Suppose ω^i for $i \in \mathbb{I}_{\bar{i}}$ are distinct, ε in (3) is sufficiently small, and the following conditions hold:*

$$Mv^i = j\omega^i v^i, \quad v^i := e^{j\theta^i} \in \mathbb{C}^n, \quad i \in \mathbb{I}_{\bar{i}},$$
$$\mathrm{eig}(M) \backslash \{j\omega^i : \ i \in \mathbb{I}_{\bar{i}}\} \subset \mathbb{C}^-.$$

Then each of the periodic signals ζ^i in (9) is a stable limit cycle of the network system (5).

Proof. From Lemma 4, we need to prove that each A^i in (25) has all its eigenvalues in the open left half plane except for one at the origin. Without loss of generality, we prove this for an arbitrarily fixed value of $i \in \mathbb{I}_{\bar{i}}$, denoted by $i = o$. The matrix $\mathsf{A}^{\underline{o}}$ constrains two terms, $\mathsf{M} - \omega^{\underline{o}}\mathsf{J}$ and $\varepsilon\mathsf{J}\mathcal{M}\mathsf{G}^{\underline{o}}$. The latter term can be regarded as a perturbation on the former. Since $\mathsf{M} - \omega^{\underline{o}}\mathsf{J}$ is the real form of $M - j\omega^{\underline{o}} I$, it has all the eigenvalues in the open left half plane except for those at $\pm j(\omega^i - \omega^{\underline{o}})$, $i \in \mathbb{I}_{\bar{i}}$ due to Lemma 5. Due to continuity of the eigenvalues, those in the open left half plane will remain there when ε is sufficiently small. Hence, it suffices to show that all the eigenvalues on the imaginary axis, except for one at the origin, will be perturbed and moved towards left by the effect of $\varepsilon\mathsf{J}\mathcal{M}\mathsf{G}^{\underline{o}}$.

Let $i \in \mathbb{I}_{\bar{i}}$. Notice that v^i is the (right) eigenvector of M associated with the eigenvalue at $j\omega^i$. Denote by u^i the corresponding left eigenvector with a normalization, that is,

$$(u^i)^* M = j\omega^i (u^i)^*, \quad (u^i)^* v^i = 1.$$

We then have

$$\begin{matrix} K^{\underline{o}} v^i = j(\omega^i - \omega^{\underline{o}})v^i, \\ (u^i)^* K^{\underline{o}} = j(\omega^i - \omega^{\underline{o}})(u^i)^*, \end{matrix} \qquad K^{\underline{o}} := M - j\omega^{\underline{o}} I.$$

It can be verified from Lemma 5 that the real form of $K^{\underline{o}}$, denoted by $\mathcal{K}^{\underline{o}}$, satisfies

$$\begin{matrix} \mathcal{K}^{\underline{o}} \mathcal{v}^i = j(\omega^i - \omega^{\underline{o}})\mathcal{v}^i, \\ (\mathfrak{u}^i)^* \mathcal{K}^{\underline{o}} = j(\omega^i - \omega^{\underline{o}})(\mathfrak{u}^i)^*, \end{matrix} \qquad \mathcal{K}^{\underline{o}} := \mathsf{M} - \omega^{\underline{o}}\mathsf{J}$$

for all $i \in \mathbb{I}_{\bar{i}}$, where

$$\mathcal{v}^i := \begin{bmatrix} v^i \\ -jv^i \end{bmatrix}, \quad \mathfrak{u}^i := \frac{1}{2}\begin{bmatrix} u^i \\ -ju^i \end{bmatrix}, \quad (\mathfrak{u}^i)^* \mathcal{v}^i = 1.$$

First, we consider the case $i \neq o$, where $j(\omega^i - \omega^{\underline{o}})$ is a simple nonzero eigenvalue of $\mathcal{K}^{\underline{o}}$ since ω^i for $i \in \mathbb{I}_{\bar{i}}$ are distinct. In light of Lemma 6, this eigenvalue of $\mathsf{A}^{\underline{o}} := \mathcal{K}^{\underline{o}} + \varepsilon\mathsf{J}\mathcal{M}\mathsf{G}^{\underline{o}}$ at $\varepsilon = 0$ is perturbed into the open left half plane with a small $\varepsilon > 0$ if $\Re((\mathfrak{u}^i)^* \mathsf{J}\mathcal{M}\mathsf{G}^{\underline{o}} \mathcal{v}^i) < 0$. A straightforward calculation shows that this is indeed the case since $(\mathfrak{u}^i)^* \mathsf{J}\mathcal{M}\mathsf{G}^{\underline{o}} \mathcal{v}^i = -\omega^i/2$.

Next, we consider the case $i = o$, where $\mathcal{K}^{\underline{o}}$ has an eigenvalue at the origin, repeated twice, which can be seen from $\mathcal{K}^{\underline{o}} \mathcal{v}^{\underline{o}} = \mathcal{K}^{\underline{o}} \bar{\mathcal{v}}^{\underline{o}} = 0$ since $\mathcal{K}^{\underline{o}}$ is real. The eigenvalue is semisimple with two linearly independent eigenvectors $\mathcal{v}^{\underline{o}}$ and $\bar{\mathcal{v}}^{\underline{o}}$ because the linear dependence implies $v^{\underline{o}} = 0$ which cannot be the case due to the supposition. To examine how this eigenvalue is perturbed, let us calculate

$$\nabla := \begin{bmatrix} \mathfrak{u}^{\underline{o}} & \bar{\mathfrak{u}}^{\underline{o}} \end{bmatrix}^* \mathsf{J}\mathcal{M}\mathsf{G}^{\underline{o}} \begin{bmatrix} \mathcal{v}^{\underline{o}} & \bar{\mathcal{v}}^{\underline{o}} \end{bmatrix} = -\frac{\omega^{\underline{o}}}{2}\begin{bmatrix} 1 & 1 \\ 1 & 1 \end{bmatrix},$$

where we noted that

$$\Theta^{\underline{o}} = C^{\underline{o}} + jS^{\underline{o}} = \mathrm{diag}(e^{j\theta^{\underline{o}}}), \quad (\Theta^{\underline{o}})^2 \bar{v}^{\underline{o}} = v^{\underline{o}}.$$

Since the eigenvalues of ∇ are $-\omega^{\underline{o}}$ and 0, Lemma 6 implies that one of the zero eigenvalues of $\mathsf{A}^{\underline{o}} := \mathcal{K}^{\underline{o}} + \varepsilon\mathsf{J}\mathcal{M}\mathsf{G}^{\underline{o}}$ at $\varepsilon = 0$ is perturbed into the open left half plane for small $\varepsilon > 0$. The direction of the perturbation for the other zero eigenvalue depends on the higher order derivatives and cannot be determined by Lemma 6. However, one can confirm that it stays at the origin because $\mathsf{A}^{\underline{o}} \Im(\mathcal{v}^{\underline{o}}) = 0$ holds for all ε. ■

The result in Theorem 2 makes intuitive sense. When ε is sufficiently small, the nonlinear element ϕ is approximately constant, $\phi(|z|) \approx 1$, in the neighborhood of each orbit ($|z| \approx \gamma$). Hence the nonlinear system (5) behaves like a linear system $\dot{z} = Mz$ in the neighborhood of each orbit. When the conditions in Theorem 2 are satisfied, the linear system $\dot{z} = Mz$ has $\mathring{\imath}$ oscillatory modes $z = \zeta^i$, and every state trajectory converges to a linear combination of these modes, where the coefficients depend on the initial condition. Theorem 2 shows that the system (5) retains the multiple oscillatory modes, and the nonlinear dynamics in $\dot{z} = M\psi(z)$ stabilize every orbit of ζ^i with guaranteed local convergence.

Based on Theorem 2, the network connection matrix M can be calculated by specifying its eigenvalues and eigenvectors in accordance with the desired oscillations. In particular, $\mathring{\imath}$ limit cycles specified by $(\omega^i, \theta^i) \in \mathbb{R} \times \mathbb{R}^n$, $i \in \mathbb{I}_{\mathring{\imath}}$ can be embedded in a network with n ($\geq \mathring{\imath}$) units by

$$\begin{aligned} &M = V\Lambda V^{-1}, \\ &V := \left[\begin{array}{cc} V_1 & V_2 \end{array}\right], \quad V_1 := \left[\begin{array}{ccc} e^{j\theta^{\underline{1}}} & \cdots & e^{j\theta^{\mathring{\imath}}} \end{array}\right] \\ &\Lambda := \mathrm{diag}(\Lambda_1, \Lambda_2), \quad \Lambda_1 := \mathrm{diag}(j\omega^{\underline{1}}, \ldots, j\omega^{\mathring{\imath}}), \end{aligned} \tag{26}$$

where V_2 is an arbitrary matrix such that V is square invertible and Λ_2 is an arbitrary Hurwitz matrix. Note that the condition requires that the number of units n must be greater than or equal to the number of target limit cycles $\mathring{\imath}$.

The following simple example illustrates how multiple limit cycles can be embedded in the state space and provides some idea about the size of the domain of attraction for each orbit.

Example 3. Consider a simple network with two oscillator units, i.e., $n = 2$. Let the target limit cycles be (9) with

$$\theta^{\underline{1}} = \left[\begin{array}{c} 0 \\ \alpha \end{array}\right], \quad \theta^{\underline{2}} = \left[\begin{array}{c} 0 \\ \beta \end{array}\right].$$

If we assume $\omega^{\underline{1}} \neq \omega^{\underline{2}}$ to satisfy the supposition in Theorem 2, it necessitates that $e^{j\alpha} \neq e^{j\beta}$. The connectivity matrix M such that $Me^{j\theta^i} = j\omega^i e^{j\theta^i}$ is then uniquely determined as

$$M = \frac{j}{e^{j\beta} - e^{j\alpha}} \left[\begin{array}{cc} \omega^{\underline{1}} e^{j\beta} - \omega^{\underline{2}} e^{j\alpha} & \omega^{\underline{2}} - \omega^{\underline{1}} \\ (\omega^{\underline{1}} - \omega^{\underline{2}}) e^{j(\alpha+\beta)} & \omega^{\underline{2}} e^{j\beta} - \omega^{\underline{1}} e^{j\alpha} \end{array}\right]$$

When the target oscillations share the same frequency $\omega^{\underline{1}} = \omega^{\underline{2}}$, then M becomes diagonal, and the two oscillators are disconnected, resulting in loss of coordination and orbital stability. When the target frequencies are distinct $\omega^{\underline{1}} \neq \omega^{\underline{2}}$, orbital stability is guaranteed as in Theorem 2 for each ζ^i.

The system (5) is simulated for the case

$$\gamma = 1, \quad \omega^{\underline{1}} = 1, \quad \omega^{\underline{2}} = 2, \quad \alpha = \pi/2, \quad \beta = -\pi/8,$$

and ϕ in (2) with $\mu = 0.1$. The trajectories resulting from several initial states are plotted in a 3-dimensional cross section of the 4-dimensional state space in Fig. 4 (left). We see that, depending on the initial condition (marked by "star"), each trajectory converges to $\zeta^{\underline{1}}$ (red) or $\zeta^{\underline{2}}$ (blue), clearly indicating co-existence of two stable limit cycles. In these coordinates, the blue and red trajectories are mingled and it is difficult to visualize the domain of attraction. Let us introduce new coordinates (r_1, r_2, d, b) defined by

$$z_1 = r_1 e^{j(b-d)/2}, \quad z_2 = r_2 e^{j(b+d)/2}.$$

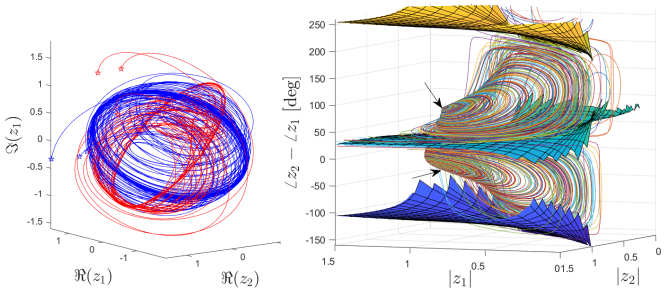

Fig. 4. Two-oscillator network with two limit cycles. Sample trajectories illustrate convergence to different orbits depending on the initial state (left). Numerically estimated domains of attraction and some example trajectories with the initial state just above and below the green surface (right).

It can be shown that (5) is then described as

$$\dot{\hat{z}} = f(\hat{z}), \quad \dot{b} = g(\hat{z}), \quad \hat{z} := (r_1, r_2, d)$$

for some functions f and g. Thus, the phase bias b does not affect the other variables, and the convergence of $\hat{z}$ to the target orbits (or equilibria in these coordinates) $\hat{\zeta}^{\underline{1}} = (\gamma, \gamma, \alpha)$ and $\hat{\zeta}^{\underline{2}} = (\gamma, \gamma, \beta)$ can be examined in the 3-dimensional state space $\hat{z} \in \mathbb{R}^3$. Some heuristic calculations (gridding the parameter space of $\hat{z}(0)$ and bisection searches for the boundaries) yielded estimates of the domain of attraction in the (r_1, r_2, d) space as shown in Fig. 4 (right).

The numerical result suggests the following. When $\hat{z}(0)$ is in the region between the green and yellow surfaces, the trajectory converges to $(1, 1, \pi/2)$ except when $\hat{z}(0)$ is close to the surfaces or the planes $r_1 = 0$ and $r_2 = 0$. In these exceptional cases, the trajectory converges to $(1, 1, \pi/2 + 2n\pi)$ for some nonzero integer n. Similarly, the region between the green and blue surfaces is the estimated domain of attraction for $\hat{z} = (1, 1, -\pi/8 + 2n\pi)$. Thus, the domain of attraction is fairly large for each target orbit although the theory guarantees local convergence only, and the actual convergence of z to the orbit of $\zeta^{\underline{1}}$ (resp. $\zeta^{\underline{2}}$) occurs when the initial phase difference $d(0)$ is close to α (resp. β), as expected.

When the oscillator is used as part of a feedback controller as in Fig. 1, plant disturbances and sensor/communication noises would perturb the state trajectory away from the targeted limit cycle orbits. The ability to return to the orbit depends on the size and shape of the domain of attraction. Example 3 shows an encouraging result for a simple oscillator where the domains of attraction divide the state space almost equally for the targeted orbits, indicating some robustness against amplitude perturbations. In addition, it suggests strong regulation of the phase for maintaining an orbit, or intentional phase perturbation for switching from one orbit to another.

V. Distributed Oscillator Network Design

A. Approach

The oscillator network design in the previous section imposes no constraints on the interconnections of the oscillators, and direct communications are allowed between any pair of oscillators, i.e., the connectivity matrix M in (5) can be fully populated with nonzero entries. This section addresses the

issue of the communication constraint and solves Problem 1 to enforce a distributed network architecture as in (7).

Our approach is the following. Partition the target phase as $\theta^i = \mathrm{col}(\theta^i_1, \ldots, \theta^i_{\mathring{\kappa}})$ where $\theta^i_k \in \mathbb{R}^{n_k}$ corresponds to the phases for the k^{th} subsystem. Decompose it into $\theta^i_k = \vartheta^i_k + \sigma^i_k$, where $\vartheta^i_k \in \mathbb{R}^{n_k}$ specifies the relative phases within the subsystem, and $\sigma^i_k \in \mathbb{R}$ specifies the global phase of the subsystem. The idea is to first design the subsystems F_k with phases ϑ^i_k, and then design the coupling $\ell_{kl}G_{kl}$ between subsystems to achieve coordination with phases σ^i_k. The first step can be executed using Theorem 2 with $M = F_k$ and $\theta^i = \vartheta^i_k$. In this case, $n_k \geq \mathring{\imath}$ is required, i.e., the dimension of each subsystem must be larger than or equal to the number of limit cycles. For the second step, we will gain insights from the single limit cycle case $\mathring{\imath} = 1$, and generalize the result to the multiple limit cycle case $\mathring{\imath} \geq 1$ in the sections that follow.

B. Network Design with Single Limit Cycle

Let us first consider the simple case where there is a single target oscillation ($\mathring{\imath} = 1$) described by (13), each subsystem is given by $F_k = j\omega$ with $n_k = 1$, and the number of subsystems is $\mathring{\kappa} = n$. In this case, the target phases are set such that $\vartheta^i_k = 0$ without loss of generality, and $\sigma^i_k = \theta_k$ where $\theta_k \in \mathbb{R}$ is the k^{th} entry of $\theta \in \mathbb{R}^n$. From Theorem 1, condition (iii), the network system described by scalars $z_k(t) \in \mathbb{C}$ satisfying

$$\dot{z}_k = j\omega\psi(z_k) - \sum_{l=1}^{\mathring{\kappa}} \ell_{kl} e^{j(\theta_k - \theta_l)}\psi(z_l), \quad k \in \mathbb{I}_{\mathring{\kappa}} \tag{27}$$

has stable limit cycle $z_k(t) = \gamma e^{j(\omega t + \theta_k)}$ if L is real and $L \in \mathbb{L}$, where L is the matrix with (k,l) entry being ℓ_{kl}. Comparing this system with (7), the coupling parameter G_{kl} can be chosen as $G_{kl} = e^{j(\theta_k - \theta_l)}$. To choose $L \in \mathbb{L}$ with a distributed structure, let us introduce the set of real square matrices L such that $L\mathbf{1} = 0$, the off-diagonal entries of L are nonpositive, and L is the Laplacian matrix of a directed graph containing a spanning tree. We denote this set by $\mathbb{L}_s$. It is well known (Lemma 3.3, [27]) that $\mathbb{L}_s \subset \mathbb{L}$ holds, which allows us to choose a structured $L \in \mathbb{L}$. Thus a solution to Problem 1 for the single limit cycle case ($\mathring{\imath} = 1$) with $n_k = 1$ is given by (7) with

$$F_k = j\omega, \quad G_{kl} = e^{j(\theta_k - \theta_l)}, \quad L \in \mathbb{L}_s.$$

Note that $L \in \mathbb{L}_s$ can be constructed by selecting arbitrary negative numbers $\ell_{kl} \in \mathbb{R}$ for $l \in \mathbb{N}_k$, and setting

$$\ell_{kk} = \sum_{l \in \mathbb{N}_k} |\ell_{kl}|, \quad \ell_{kl} = 0, \quad l \notin \check{\mathbb{N}}_k, \tag{28}$$

provided the neighbor sets $\mathbb{N}_k$ for $k \in \mathbb{I}_{\mathring{\kappa}}$ define a directed graph containing a spanning tree. The following example illustrates this design method.

Example 4. Consider the network of four-unit oscillators with the connectivity specified by the Laplacian matrix

$$L = \begin{bmatrix} -1 & 0 & 1 & 0 \\ 1 & -1 & 0 & 0 \\ 1 & 0 & -1 & 0 \\ 0 & 0 & 1 & -1 \end{bmatrix}.$$

The network is illustrated in Fig. 5. The edges highlighted in red form a spanning tree with vertex 1 being the root. The nonzero off-diagonal entries are negative, and each row sums up to zero. Thus $L \in \mathbb{L}_s$. We consider the target limit cycle with phase $\theta = \mathrm{col}(0, \pi/3, 2\pi/3, \pi)$, frequency $\omega = 2\pi$, and amplitude $\gamma = 1$. The simulation result in Fig. 5 shows convergence to the target as theoretically guaranteed.

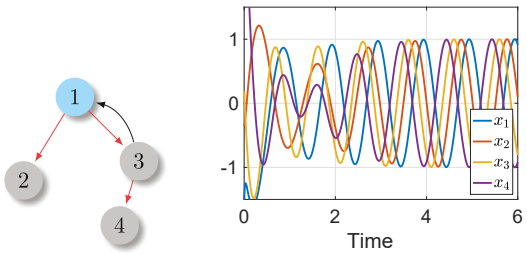

Fig. 5. Network structure and simulated response of $x_k := \Re(z_k)$.

C. Network Design with Multiple Limit Cycles

We now extend the result of the previous section to the case where there are multiple target oscillations. The insight from the single target case is that the network specified by L should have a spanning tree with positive weights, and the coupling parameter G_{kl} should be chosen to satisfy $G_{kl}\zeta^i_l = \zeta^i_k$ so that the coupling is diffusive. This idea naturally extends to the following result.

Theorem 3. *Consider Problem 1. Partition the target phase as $\theta^i = \mathrm{col}(\theta^i_1, \ldots, \theta^i_{\mathring{\kappa}})$ with $\theta^i_k \in \mathbb{R}^{n_k}$, and decompose it into $\theta^i_k = \vartheta^i_k + \sigma^i_k$ with $\vartheta^i_k \in \mathbb{R}^{n_k}$ and $\sigma^i_k \in \mathbb{R}$. Let the set of $\mathring{\kappa}$ local subsystems described by (6) be given. Suppose, for each $k \in \mathbb{I}_{\mathring{\kappa}}$, the k^{th} subsystem satisfies the orbital stability condition in Theorem 2 with $M = F_k$ and $\theta^i = \vartheta^i_k$, and has $\mathring{\imath}$ stable limit cycle(s)*

$$z_k(t) = \gamma e^{j(\omega^i t + \vartheta^i_k)} \in \mathbb{C}^{n_k}, \quad i \in \mathbb{I}_{\mathring{\imath}}.$$

Let a network Laplacian matrix $L \in \mathbb{R}^{\mathring{\kappa} \times \mathring{\kappa}}$ be defined so that its (k,l) entries for $k \in \mathbb{I}_{\mathring{\kappa}}$ and $l \in \check{\mathbb{N}}_k$ are ℓ_{kl} and the other entries are zero. Then, the network system (7) has $\mathring{\imath}$ orbitally stable limit cycles $z = \zeta^i$ as specified in (9) if

$$L \in \mathbb{L}_s, \quad G_{kl}V_l = V_k, \tag{29}$$

hold for all $l \in \check{\mathbb{N}}_k$ and $k \in \mathbb{I}_{\mathring{\kappa}}$, where

$$V_k := \begin{bmatrix} v^1_k & \cdots & v^{\mathring{\imath}}_k \end{bmatrix} \in \mathbb{C}^{n_k \times \mathring{\imath}}, \quad v^i_k := e^{j(\vartheta^i_k + \sigma^i_k)}.$$

Proof. Since the subsystem $\dot{z}_k = F_k\psi(z_k)$ satisfies the orbital stability condition in Theorem 2, we have

$$F_kV_k = V_k\Lambda, \quad \Lambda := \mathrm{diag}(j\omega^1, \ldots, j\omega^{\mathring{\imath}}).$$

Note that V_k has a full column rank because its columns are the eigenvectors of F_k associated with distinct eigenvalues $j\omega^i$. We will prove the case $n_k > \mathring{\imath}$; the case $n_k = \mathring{\imath}$ can be shown similarly. Let U_k be a matrix such that

$$\begin{bmatrix} V^\dagger_k \\ U^\dagger_k \end{bmatrix} \begin{bmatrix} V_k & U^\dagger_k \end{bmatrix} = I.$$

We then have

$$\left[\begin{array}{c} V_k^\dagger \\ U_k \end{array}\right] F_k \left[\begin{array}{cc} V_k & U_k^\dagger \end{array}\right] = \left[\begin{array}{cc} \Lambda & * \\ 0 & \Omega_k \end{array}\right], \quad \Omega_k := U_k F_k U_k^\dagger.$$

Since each subsystem satisfies the condition in Theorem 2, Ω_k is Hurwitz. The coupled oscillators can be described by

$$\begin{array}{ll} \dot{z} = M\psi(z), & z := \mathrm{col}(z_1, \ldots, z_{\mathring{\kappa}}), \\ M := F - G, & F := \mathrm{diag}(F_1, \ldots, F_{\mathring{\kappa}}), \end{array} \tag{30}$$

where G is a matrix with its (k,l) block given by $\ell_{kl} G_{kl}$. It can readily be verified that

$$\begin{array}{lll} FV = V\Lambda, & GV = V\mathcal{L}, & V := \mathrm{diag}(V_1, \ldots, V_{\mathring{\kappa}}), \\ UF = \Omega U, & UG = 0, & U := \mathrm{diag}(U_1, \ldots, U_{\mathring{\kappa}}), \\ \Lambda := I \otimes \Lambda, & \mathcal{L} := L \otimes I, & \Omega := \mathrm{diag}(\Omega_1, \ldots, \Omega_{\mathring{\kappa}}), \end{array}$$

from which we obtain

$$M\mathcal{V} = \mathcal{V}\Lambda, \quad \mathcal{V} := \mathrm{col}(V_1, \ldots, V_k),$$

$$\left[\begin{array}{c} V^\dagger \\ U \end{array}\right] M \left[\begin{array}{cc} V & U^\dagger \end{array}\right] = \left[\begin{array}{cc} \Lambda - \mathcal{L} & * \\ 0 & \Omega \end{array}\right],$$

where $G\mathcal{V} = 0$ follows from $L\mathbf{1} = 0$. From Lemma 6 in [12], due to $L \in \mathbb{L}_s$, the set of eigenvalues of $\Lambda - \mathcal{L}$ contains the eigenvalues of Λ, and all the remaining eigenvalues have negative real parts. Thus the coupled oscillator network satisfies $M\nu^i = j\omega^i \nu^i$ for each $i \in \mathbb{I}_{\mathring{\imath}}$ where ν^i is the i^{th} column of $\mathcal{V}$, and all the eigenvalues of M except for those of Λ are in the open left half plane. Therefore, by Theorem 2, $z(t) = \gamma \nu^i e^{j\omega^i t}$ for $i \in \mathbb{I}_{\mathring{\imath}}$ are orbitally stable limit cycles of the network. ■

From Theorem 2, the network design boils down to the search for the coupling matrix M such that it has a set of eigenvalues and eigenvectors specifying the target oscillations, and the rest of eigenvalues in the open left half plane. When the network is required to have a distributed architecture, a structural constraint is placed on M. Thus the essential problem is to find a structured matrix M with a prescribed eigenstructure. Theorem 3 provides a solution in terms of diffusively coupled subsystems. Condition $G_{kl} V_l = V_k$ implies $G_{kl}\psi(\zeta_l^i) = \psi(\zeta_k^i)$ and thus the second term in (7) vanishes on the target orbit due to $L\mathbf{1} = 0$.

The distributed design of M in Theorem 3 results in lower computational complexity than the design of networks with all-to-all interactions as in Theorem 2. The latter involves an inversion of an $n \times n$ matrix as in (26) for an n-unit network, requiring $O(n^3)$ arithmetic operations. In contrast, the former requires calculations of intra-subsystem coupling matrices $F_k \in \mathbb{C}^{n_k \times n_k}$ for $k \in \mathbb{I}_{\mathring{\kappa}}$ and inter-subsystem coupling matrices $G_{kl} \in \mathbb{C}^{n_k \times n_l}$ satisfying (29) for all connected edges $\{(k,l) : k \in \mathbb{I}_{\mathring{\kappa}}, l \in \check{\mathbb{N}}_k\}$. The computational complexity for these is $O(n^3/\mathring{\kappa}^2)$ assuming $n_k = n/\mathring{\kappa}$ for all $k \in \mathbb{I}_{\mathring{\kappa}}$ (same dimension for all subsystems) and $|\check{\mathbb{N}}_k| = O(1)$ (the number of neighbors for each subsystem is fixed). Thus, clustering into $\mathring{\kappa}$ subsystems with local interactions reduces the computational complexity by the factor of $1/\mathring{\kappa}^2$.

Coupling of the subsystems through aggregated signals would reduce the dimension of the signals transmitted between subsystems, thereby reducing the load on the communication channels. In our formulation, the inter-subsystem coupling can be aggregated through a factorization of G_{kl}. Specifically, a solution G_{kl} to (29) always exists because V_l has a full column rank, and $G_{kl} = V_k V_l^\dagger$ is a solution. In this case, it suffices to "broadcast" the aggregate signal $\hbar_l := V_l^\dagger \psi(z_l)$ from the l^{th} subsystem to its neighbors. The signal $\ell_{kl} G_{kl} \psi(z_l)$ needed for the coupling as in (7) can then be constructed at the k^{th} subsystem as $\ell_{kl} V_k \hbar_l$. The dimension of $\hbar_l$ is $\mathring{\imath}$, the number of limit cycles to be embedded in the network. Note in particular that, if $\mathring{\imath} = 1$ and the synchronization is targeted ($V_k = \mathbf{1}$ for all $k \in \mathbb{I}_{\mathring{\kappa}}$), then the transmission signal would be the average ($\hbar_l = \mathbf{1}^{\mathrm{T}} \psi(z_l)/n_l$) and the same input $\ell_{kl} \hbar_l$ is applied to all n_k units in the k^{th} subsystem, which is a commonly used "cluster-control" protocol for synchronization (e.g. [53]).

VI. A Comprehensive Design Example

This section provides a design example of an oscillator network with a constraint on the communication topology, possessing two limit cycle orbits from which periodic outputs of arbitrary temporal shapes are generated. We use human motion data from [54], which contains time history of the hip, knee, and ankle joints during a period of human locomotion. Here we pick two sets of gait data, one for running at 2.6 m/s, another for walking at 1.6 m/s. We will design a distributed network of oscillators to produce the two gaits.

Consider two gaits $\eta^i(t) \in \mathbb{R}^6$ for walking $(i = 1)$ and running $(i = 2)$, where the six entries of η^i are ordered as LA, LK, LH, RH, RK, RA with L and R indicating left and right, and A, K, H indicating ankle, knee, and hip. The data for the left leg is shown by the solid curves in Fig. 6, while the data for the right leg is assumed 180° out of phase with respect to the left leg. Take the Fourier series approximations

$$\eta^i(t) \approx \tilde{\eta}^i(t) := \sum_{l=0}^{\ell^i} \Re[\hat{\eta}_l^i e^{jl\omega^i t}], \quad i = 1, 2$$

where $\hat{\eta}_l^i \in \mathbb{C}^6$ are the Fourier coefficients for the i^{th} gait, the fundamental frequencies are

$$\omega^{\underline{1}} = 5.53 \text{ rad/s}, \quad \omega^{\underline{2}} = 8.93 \text{ rad/s},$$

and we choose $\ell^i = 3$ for $i = 1, 2$, which give reasonable approximations, as indicated by the dashed curves in Fig. 6. Let us use the phase of the fundamental harmonic component, $\varrho^i := \angle(\hat{\eta}_1^i) \in \mathbb{R}^6$, as the reference phase of the basis function for temporal shaping, and express the target output as

$$\tilde{\eta}^i(t) = \sum_{l=0}^{3} \Re\Big(c_l^i \cdot e^{j(\omega^i t + \varrho^i)l}\Big), \quad i = 1, 2$$

where $c_l^i := \hat{\eta}_l^i \cdot e^{-jl\varrho^i}$.

We design a network consisting of six ($\mathring{\kappa} = 6$) subsystems, each of which produces scalar output $y_k(t) \in \mathbb{R}$, $k \in \mathbb{I}_{\mathring{\kappa}}$, so that the collective output $y(t) \in \mathbb{R}^{\mathring{\kappa}}$ converges to the orbit of $\tilde{\eta}_1$ or $\tilde{\eta}_2$. The network is described by (7) with output signals $y_k = h_k(z_k)$. We use the static nonlinearity ψ specified in (1) with (2). The parameters F_k, G_{kl}, ℓ_{kl} and functions h_k should be determined for $k, l \in \mathbb{I}_{\mathring{\kappa}}$ so that the network has two ($\mathring{\imath} = 2$) stable limit cycles on which $y_k = \tilde{\eta}_k^i$ holds for $i \in \mathbb{I}_{\mathring{\imath}}$ and $k \in \mathbb{I}_{\mathring{\kappa}}$.

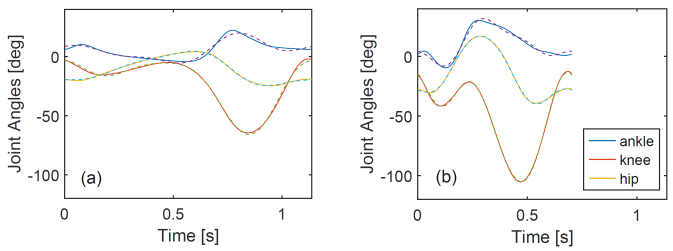

Fig. 6. Two gaits of locomotion: (a) walking at 1.6 m/s, (b) running at 2.6 m/s. The solid curves are kinematic variables of human motion data [54]. The dashed curves are Fourier series approximations.

The network topology follows that of human legs as shown in Fig. 7. Each subsystem is coupled with its nearest neighbors, and the topology is captured by the Laplacian matrix $L \in \mathbb{R}^{6\times 6}$ specified by $L\mathbf{1} = 0$ and its (k,l) entries

$$\ell_{kl} = \begin{cases} -1, & (|k-l| = 1), \\ 0, & (|k-l| \geq 2). \end{cases}$$

For each leg joint, a subsystem with two-unit oscillators is used ($n_k = 2$) to meet the requirement $n_k \geq \mathring{\imath}$ for local subsystem design (Theorem 2) and for output shaping (Lemma 2). We consider identical subsystems, each given by $F_k = M$ with M in Example 3 where $\alpha = \pi/2$ and $\beta = \pi$. Thus we use

$$\vartheta_k^1 = \begin{bmatrix} 0 \\ \alpha \end{bmatrix}, \quad \vartheta_k^2 = \begin{bmatrix} 0 \\ \beta \end{bmatrix}, \quad k \in \mathbb{I}_{\mathring{\kappa}}$$

as the internal phases for each subsystem, and the relative phases $\sigma_k^i \in \mathbb{R}$ between subsystems are set from the k^{th} entry of the gait data $\sigma_k^i := \varrho_k^i$. The target limit cycles for the network oscillator design are given by (9) with $\gamma = 1$, $\theta^i = \text{col}(\theta_1^i, \ldots, \theta_6^i)$, and $\theta_k^i := \vartheta_k^i + \sigma_k^i \in \mathbb{R}^{n_k}$. From Theorem 3, V_k in (29) are 2×2 invertible matrices, and we have $G_{kl} = V_k V_l^{-1}$. The structured network connection matrix M can then be constructed as in (30). The eigenvalues of M are given by $-a + j\omega$ for the 12 combinations of $\omega = \omega^1, \omega^2$ and $a = 0, 1, 2, 3, \tan(\pi/12), \tan(5\pi/12)$.

The output from each subsystem can be defined from Lemma 2 and the discussion that followed. In particular, with $\varrho_k^i = \sigma_k^i \in \mathbb{R}$ and $\theta_k^i := \vartheta_k^i + \sigma_k^i \in \mathbb{R}^{n_k}$, we have

$$y_k := \sum_{i=1}^{2} \Re\Big(c_{0k}^i \, |H_k^i z_k| + \sum_{l=1}^{3} c_{lk}^i \, (H_k^i z_k)^l \Big),$$

$$H_k^1 := \begin{bmatrix} 1 & 0 \end{bmatrix} \begin{bmatrix} e^{j\vartheta_k^1} & e^{j\vartheta_k^2} \end{bmatrix}^{-1},$$
$$H_k^2 := \begin{bmatrix} 0 & 1 \end{bmatrix} \begin{bmatrix} e^{j\vartheta_k^1} & e^{j\vartheta_k^2} \end{bmatrix}^{-1},$$

where $c_{lk}^i \in \mathbb{C}$ is the k^{th} entry of $c_l^i \in \mathbb{C}^6$.

The distributed network thus designed was simulated for various initial conditions to confirm that the two limit cycles corresponding to the two gaits are embedded in the system with orbital stability. Example responses are shown in Fig. 8 where output $y(t) \in \mathbb{R}^6$ converges to different gaits $\tilde{\eta}^i$. The initial conditions $z_k(0)$ are set to zero except for the hip joints that are made anti-phase: $z_3 = -z_4 = \text{col}(a, 0)$. The output is found to converge to the walking gait when a is large (e.g. $a = 5$), and to the running gait when a is small (e.g. $a = 1/5$).

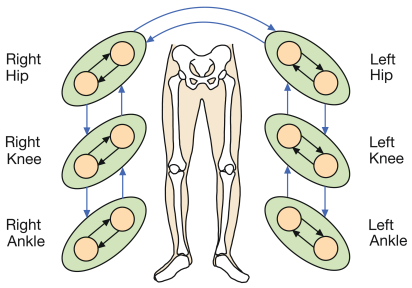

Fig. 7. Oscillator network for gait generation

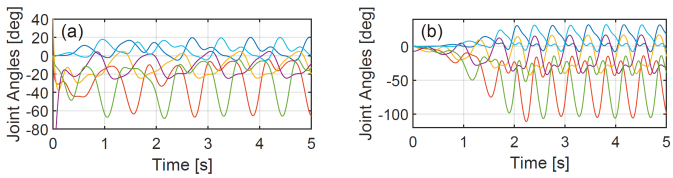

Fig. 8. Convergence to two gaits in simulated network. Time courses of $y(t) \in \mathbb{R}^6$ for walking (a) and running (b).

The transition between two gaits can be achieved by steering the state z at some point in time. This is demonstrated in Fig. 9, where, for brevity, the result is shown only for the left leg. The initial state is specified in the same way as case (b) in Fig. 8, leading to the running gait within several seconds. The dynamics of the network is modified to $\dot{z}_k = 6(\mathring{z}_k - z_k)$ during $6 < t < 6.2$ to move the state into the domain of attraction for the walking gait, where $\mathring{z}_k \in \mathbb{C}^2$ for $k \in \mathbb{I}_{\mathring{\kappa}}$ are specified as zero except for $\mathring{z}_3 = -\mathring{z}_4 = \text{col}(5, 0)$. This results in the transition to the walking gait. Also shown in Fig. 9 are the time courses of the first entries of z_k for the left leg. The network has been designed so that these variables are phase-synchronized with the gait output, which can be observed in the figure. Thus, transitions between limit cycles are possible through proper steering of the state.

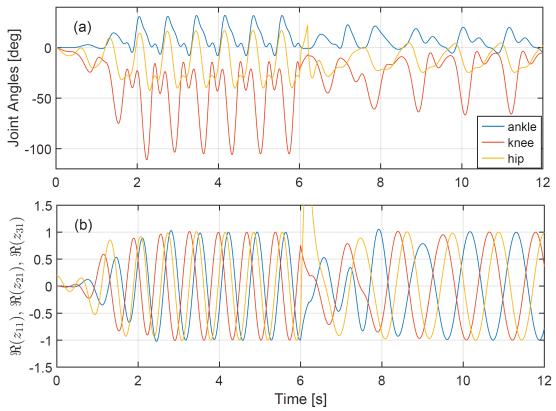

Fig. 9. Gait transition from running to walking. (a) outputs y_k for $k = 1, 2, 3$, converging to the target orbits for the left leg. (b) real parts of states z_{k1} for $k = 1, 2, 3$ which are the first entries of $z_k(t) \in \mathbb{C}^2$.

Next, we illustrate robustness of the gait generation against communication failures. The network oscillator is initiated as before and the trajectory converged to the steady running before $t = 6$ as shown in Fig. 9. The network communication

between the left ankle subsystem and all the other subsystems is cut off at $t = 6$ to emulate a possible failure. It is observed as in Fig. 10(a) that the network continued to generate the running gait with a reduced amplitude but correct frequency/phase/shape. For comparison, a network oscillator with all-to-all coupling is designed from Theorem 2 using (26) with $\mathring{\imath} = 2$, $\Lambda_2 = -I_{10}$, and $V_2 \in \mathbb{C}^{12\times 10}$ being a matrix such that $V^*V = \mathrm{diag}(*, I_{10})$, where I_{10} is the 10×10 identity matrix, and $\theta_k^i = \vartheta_k^i + \sigma_k^i$. When simulated under the same condition, the trajectory initially converges to the running gait with the transient almost identical to that of the distributed network, but the running gait cannot be maintained after the ankle failure as shown in Fig. 10(b). Thus, the distributed architecture of the oscillator network can be beneficial for robustly maintaining gait generation.

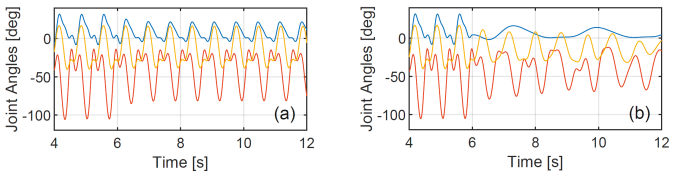

Fig. 10. Communication failure during steady running: (a) distributed network, (b) centralized network. The communications to/from the left ankle failed for the network oscillator during $t \geq 6$.

VII. Conclusion

We have proposed a systematic method for designing a distributed network that embeds multiple limit cycles with guaranteed orbital stability. It is also shown how output signals can be defined as fixed functions of the state variables so that periodic signals with desired temporal shapes can be generated approximately with an arbitrarily high accuracy. Adopting a weakly nonlinear harmonic oscillator as the basic unit, the condition for multistability of limit cycles is characterized by eigenstructure of the network connectivity matrix. The nonlinearity of the coupling is essential for encoding the frequency into the network rather than the oscillator unit.

The network has a hierarchical architecture of coupled subsystems, each of which is a subnetwork of the unit oscillators. This architecture was the key factor for enabling simultaneous satisfaction of multistability and communication constraints. Initially, we attempted to solve Problem 1 without the subnetwork architecture (i.e., $n_k = 1$), and found it difficult to achieve multiple limit cycles $\mathring{\imath} > 1$. The result presented here revealed that subsystems with dimension $n_k \geq \mathring{\imath}$ allowed for satisfaction of the internal model principle to embed $\mathring{\imath}$ limit cycles within each subsystem, making Problem 1 tractable.

Our result will be a foundation for distributed feedback control design to achieve multiple limit cycles for the closed-loop system, where the network oscillator is embedded within the feedback loop (e.g. Fig. 1), possibly with network updates through learning [55], [56]. In this case, the communication noise may be added to the signal $\hbar_l$ transmitted from the l^{th} subsystem to its neighbors (see Section V-C) in addition to the commonly considered plant disturbances and sensor noises. A full development of such design theory may lead to a new paradigm for distributed control of oscillations. Our ongoing research is directed toward such a goal.

Appendix

Lemma 5. *Let complex matrices A, B, and C be given. Then*

$$AB = C \quad \Leftrightarrow \quad A^{\mathrm{r}}B^{\mathrm{r}} = C^{\mathrm{r}}, \tag{31}$$
$$\mathrm{eig}(A) \cup \overline{\mathrm{eig}(A)} = \mathrm{eig}(A^{\mathrm{r}})$$

hold, provided the matrix dimensions are compatible.

Proof. See Lemma 3 in [48]. ■

Lemma 6. *Let $A, B \in \mathbb{R}^{n\times n}$ be given. Assume that A has a semisimple eigenvalue $\lambda_o = j\omega$, $\omega \in \mathbb{R}$ with multiplicity r, i.e., there are nonsingular matrices*

$$X = \begin{bmatrix} X_1 & X_2 \end{bmatrix} \in \mathbb{C}^{n\times n}, \quad Y = \begin{bmatrix} Y_1 & Y_2 \end{bmatrix} \in \mathbb{C}^{n\times n}$$

with $X_1, Y_1 \in \mathbb{C}^{n\times r}$ such that

$$Y^*AX = \begin{bmatrix} \lambda_o I_r & 0 \\ 0 & \Lambda \end{bmatrix}, \quad Y^*X = I, \quad \lambda_o \notin \mathrm{eig}(\Lambda),$$

where I_r is the $r \times r$ identity matrix. Let $\lambda_1(\varepsilon), \cdots, \lambda_r(\varepsilon)$ be continuous functions $\mathbb{R} \mapsto \mathbb{C}$ parametrizing r eigenvalues of $A + \varepsilon B$ such that $\lambda_i(0) = \lambda_o$ for all $i \in \mathbb{I}_r$. Then the derivatives of $\lambda_i(\varepsilon)$, $i \in \mathbb{I}_r$, at $\varepsilon = 0$ are given by the eigenvalues of

$$\nabla = Y_1^* B X_1.$$

Consequently, there exists a real scalar $\bar{\varepsilon} > 0$ such that

$$\Re(\lambda_i(\varepsilon)) < 0, \quad i \in \mathbb{I}_r,$$

holds for all $\varepsilon \in \mathbb{R}$ such that $0 < \varepsilon < \bar{\varepsilon}$ if ∇ is Hurwitz.

Proof. See Lemma 3.1 of [57]. ■

Acknowledgments

The authors would like to thank Dr. Zhiyong Chen and Dr. Minyue Fu for helpful discussions, and Dr. Martin Grimmer for providing them with numerical data of human locomotion. This work is supported by NSF 2113528.

References

[1] N. Sadegh, R. Horowitz, W. Kao, and M. Tomizuka, "A unified approach to the design of adaptive and repetitive controllers for robotic manipulators," *Trans. ASME*, vol. 112, 1990.
[2] E. Gilbert, "Vehicle cruise: Improved fuel economy by periodic control," *Automatica*, vol. 12, pp. 159–166, 1976.
[3] J. Speyer, "Periodic optimal flight," *J. Guid. Contr. Dyn.*, vol. 19, no. 4, pp. 745–755, 1996.
[4] X. Lan and M. Schwager, "Planning periodic persistent monitoring trajectories for sensing robots in Gaussian random fields," *Int. Conf. Robotics and Automation*, pp. 2415–2420, 2013.
[5] S. Pinto, S. Andersson, J. Hendrickx, and C. Cassandras, "Optimal periodic multi-agent persistent monitoring of a finite set of targets with uncertain states," *Proc. American Contr. Conf.*, pp. 5207–5212, 2020.
[6] T. Aderinto and H. Li, "Review on power performance and efficiency of wave energy converters," *Energies*, vol. 12, no. 4329, 2019.
[7] A. Ijspeert, A. Crespi, D. Ryczko, and J. Cabelguen, "From swimming to walking with a salamander robot driven by a spinal cord model," *Science*, vol. 315, no. 5817, pp. 1416–1420, 2007.
[8] A. Ijspeert, "Central pattern generators for locomotion control in animals and robots: A review," *Neural Networks*, vol. 21, pp. 642–653, 2008.

[9] A. Wu and T. Iwasaki, "Design of controllers with distributed CPG architecture for adaptive oscillations," *Int. J. Robust and Nonlin. Contr.*, vol. 31, no. 2, pp. 694–714, 2021.

[10] T. Iwasaki, J. Chen, and W. Friesen, "Biological clockwork underlying adaptive rhythmic movements," *Proc. National Academy of Sciences of USA*, vol. 111, no. 3, pp. 978–983, 2014.

[11] R. Thandiackal, K. Melo, L. Paez, J. Herault, T. Kano, K. Akiyama, F. Boyer, D. Ryczko, A. Ishiguro, and A. Ijspeert, "Emergence of robust self-organized undulatory swimming based on local hydrodynamic force sensing," *Science Robotics*, vol. 6, p. eabf6354, 2021.

[12] A. Wu and T. Iwasaki, "Pattern formation via eigenstructure assignment: General theory and multi-agent applications," *IEEE Trans. Auto. Contr.*, vol. 63, no. 7, pp. 1959–1972, 2018.

[13] R. Olfati-Saber and R. Murray, "Consensus problems in networks of agents with switching topology and time-delays," *IEEE. Trans. Auto. Contr.*, vol. 49, no. 9, pp. 1520–1533, 2004.

[14] W. Ren, "Synchronization of coupled harmonic oscillators with local interaction," *Automatica*, vol. 44, no. 12, pp. 3195–3200, 2008.

[15] L. Scardovi and R. Sepulchre, "Synchronization in networks of identical linear systems," *Automatica*, vol. 45, pp. 2557–2562, 2009.

[16] P. Wieland, R. Sepulchre, and F. Allgower, "An internal model principle is necessary and sufficient for linear output synchronization," *Automatica*, vol. 47, pp. 1068–1074, 2011.

[17] H. Kim, H. Shim, and J. H. Seo, "Output consensus of heterogeneous uncertain linear multi-agent systems," *IEEE Trans. Auto. Contr.*, vol. 56, no. 1, pp. 200–206, 2010.

[18] J. Buchli, L. Righetti, and A. J. Ijspeert, "Engineering entrainment and adaptation in limit cycle systems," *Biol. Cyb.*, vol. 95, no. 6, pp. 645–664, 2006.

[19] T. Iwasaki, "Multivariable harmonic balance for central pattern generators," *Automatica*, vol. 44, no. 12, pp. 4061–4069, 2008.

[20] L. Zhu, Z. Chen, and R. H. Middleton, "A general framework for robust output synchronization of heterogeneous nonlinear networked systems," *IEEE Trans. Auto. Contr.*, vol. 61, no. 8, pp. 2092–2107, 2015.

[21] S. Y. Shafi, M. Arcak, M. Jovanović, and A. K. Packard, "Synchronization of diffusively-coupled limit cycle oscillators," *Automatica*, vol. 49, no. 12, pp. 3613–3622, 2013.

[22] A. Pavlov, A. V. Proskurnikov, E. Steur, and N. van de Wouw, "Synchronization of networked oscillators under nonlinear integral coupling," *IFAC-PapersOnLine*, vol. 51, no. 33, pp. 56–61, 2018.

[23] A. Pogromsky, G. Santoboni, and H. Nijmeijer, "Partial synchronization: from symmetry towards stability," *Physica D*, vol. 172, pp. 65–87, 2002.

[24] W. Wang and J. Slotine, "On partial contraction analysis for coupled nonlinear oscillators," *Biol. Cyb.*, vol. 92, no. 1, pp. 38–53, 2005.

[25] G. Ermentrout and N. Kopell, "Frequency plateaus in a chain of weakly coupled oscillators, I." *SIAM J. Math. Anal.*, vol. 15, no. 2, pp. 215–237, March 1984.

[26] X. Liu and T. Iwasaki, "Design of coupled harmonic oscillators for synchronization and coordination," *IEEE Trans. Auto. Contr.*, vol. 62, no. 8, pp. 3877–3889, 2017.

[27] W. Ren and R. Beard, "Consensus seeking in multiagent systems under dynamically changing interaction topologies," *IEEE Trans. Auto. Contr.*, vol. 50, no. 5, pp. 655–661, 2005.

[28] A. Pogromsky and H. Nijmeijer, "Cooperative oscillatory behavior of mutually coupled dynamical systems," *IEEE Trans. Circ. Sys. – I: Fund. Theory and Appl.*, vol. 48, no. 2, pp. 152–162, 2001.

[29] W. Lohmiller and J. Slotine, "On contraction analysis for non-linear systems," *Automatica*, vol. 34, no. 6, pp. 683–696, 1998.

[30] Q. Pham and J. Slotine, "Stable concurrent synchronization in dynamic system networks," *Neural Networks*, vol. 20, pp. 62–77, 2007.

[31] H. Khalil, *Nonlinear Systems*. Prentice Hall, 1996.

[32] K. Rogov, A. Pogromsky, E. Steur, W. Michiels, and H. Nijmeijer, "Pattern analysis in networks of diffusively coupled Lur'e systems," *Int. J. Bifurcation and Chaos*, vol. 29, no. 14, p. 1950200, 2019.

[33] H. Amann, *Ordinary Differential Equations: An Introduction to Nonlinear Analysis*. Walter de Gruyter, 1990.

[34] L. Pecora and T. Carroll, "Master stability functions for synchronized coupled systems," *Phys. Rev. Lett.*, vol. 80, no. 10, pp. 2109–2112, 1998.

[35] S. Hara, H. Tanaka, and T. Iwasaki, "Stability analysis of systems with generalized frequency variables," *IEEE Trans. Auto. Contr.*, vol. 59, no. 2, pp. 313–326, 2014.

[36] E. Izhikevich and Y. Kuramoto, "Weakly coupled oscillators," *Encyclopedia of Mathematical Physics, Elsevier*, vol. 5, p. 448, 2006.

[37] Y. Kuramoto, "Self-entrainment of a population of coupled non-linear oscillators," *Int. Sympo. Math. Prob. in Theor. Phys.*, pp. 420–422, 1975.

[38] F. Dorfler and F. Bullo, "Synchronization in complex networks of phase oscillators: A survey," *Automatica*, vol. 50, pp. 1539–1564, 2014.

[39] B. Ermentrout, Y. Park, and D. Wilson, "Recent advances in coupled oscillator theory," *Phil. Trans. R. Soc. A*, vol. 377, p. 20190092, 2019.

[40] G. Taga, "Self-organized control of bipedal locomotion by neural oscillators in unpredictable environment," *Biol. Cybern.*, vol. 65, no. 3, pp. 147–159, 1991.

[41] C. P. Santos and V. Matos, "Gait transition and modulation in a quadruped robot: A brainstem-like modulation approach," *Robotics and Autonomous Systems*, vol. 59, no. 9, pp. 620–634, 2011.

[42] S. Inagaki, H. Yuasa, and T. Arai, "CPG model for autonomous decentralized multi-legged robot system – generation and transition of oscillation patterns and dynamics of oscillators," *Robotics and Autonomous Systems*, vol. 44, no. 3-4, pp. 171–179, 2003.

[43] Z. Bing, L. Cheng, G. Chen, F. Rohrbein, K. Huang, and A. Knoll, "Towards autonomous locomotion: CPG-based control of smooth 3d slithering gait transition of a snake-like robot," *Bioinspiration & Biomimetics*, vol. 12, p. 035001, 2017.

[44] G. Schöner, W. Jiang, and J. Kelso, "A synergetic theory of quadrupedal gaits and gait transitions," *J. Theor. Biol.*, vol. 142, pp. 359–391, 1990.

[45] M. Golubitsky, I. Stewart, P. Buono, and J. Collins, "Symmetry in locomotor central pattern generators and animal gaits," *Nature*, vol. 401, no. 6754, pp. 693–695, 1999.

[46] A. Ijspeert, A. Crespi, and J. Cabelguen, "Simulation and robotics studies of salamander locomotion," *Neuroinformatics*, vol. 3, pp. 171–195, 2005.

[47] S. Suzuki, T. Kano, A. Ijspeert, and A. Ishiguro, "Spontaneous gait transitions of sprawling quadruped locomotion by sensory-driven body-limb coordination mechanisms," *Frontiers in Neurorobotics*, vol. 15, p. 645731, 2021.

[48] K. Ren and T. Iwasaki, "Design of complex oscillator network with multiple limit cycles," *Proc. IEEE Conf. Dec. Contr.*, 2018.

[49] L. Righetti and A. Ijspeert, "Programmable central pattern generators: an application to biped locomotion control," *IEEE Int. Conf. Robotics and Automation*, pp. 1585–1590, 2006.

[50] S. Kohannim and T. Iwasaki, "Design of coupled Andronov-Hopf oscillators with desired strange attractors," *Nonlinear Dynamics*, vol. 100, no. 2, pp. 1659–1672, 2020.

[51] J. Hauser and C. Chung, "Converse Lyapunov functions for exponentially stable periodic orbits," *Sys. Contr. Lett.*, vol. 23, pp. 27–34, 1994.

[52] P. Hartman, *Ordinary Differential Equations*. John Wiley&Sons, 1964.

[53] D. Uzhva and O. Granichin, "Cluster control of complex cyber-physical systems," *Cybernetics and Physics*, vol. 10, no. 3, pp. 191–200, 2021.

[54] M. Grimmer, A. A. Elshamanhory, and P. Beckerle, "Human lower limb joint biomechanics in daily life activities: a literature based requirement analysis for anthropomorphic robot design," *Front. in Robo. AI*, 2020.

[55] L. Righetti, J. Buchli, and A. Ijspeert, "Dynamic Hebbian learning in adaptive frequency oscillators," *Physica D: Nonlinear Phenomena*, vol. 216, no. 2, pp. 269–281, 2006.

[56] J. Zhao and T. Iwasaki, "CPG control for harmonic motion of assistive robot with human motor control identification," *IEEE Trans. Contr. Sys. Tech.*, vol. 28, no. 4, pp. 1323–1336, 2019.

[57] M. Overton and R. Womersley, "On minimizing the spectral radius of a nonsymmetric matrix function: Optimality conditions and duality theory," *SIAM J. Matrix Anal. Appl.*, vol. 9, no. 4, pp. 473–498, 1988.

Kewei Ren received a B.S. degree in Aerospace engineering from Beihang University, and a Ph.D. degree in Aerospace Engineering from the University of California, Los Angeles, in 2015 and 2021, respectively. He currently works at Momenta as an engineer on motion planning and trajectory optimization.

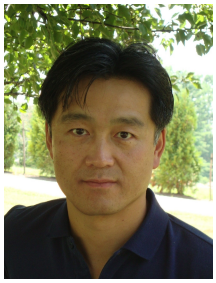

Tetsuya Iwasaki (M'90-SM'01-F'09) received his B.S. and M.S. degrees in Electrical Engineering from the Tokyo Institute of Technology in 1987 and 1990, and his Ph.D. degree in Aeronautics and Astronautics from Purdue University in 1993. He held faculty positions at Tokyo Tech and University of Virginia before joining the UCLA. His research interests include control, oscillation, locomotion, and pattern formation. He has received awards from NSF, SICE, IEEE, ASME, and others. He has served as Senior/Associate Editor of several control journals.